Sensors & Diagnostics

CRITICAL REVIEW

View Article Online
View Journal

Check for updates

Cite this: DOI: 10.1039/d5sd00176e

Microfluidic platforms for CRISPR-based biosensing advancing molecular diagnostics from benchtop to point-of-care

Yanping Wang, †[a] Huimin Jiang,†[a] Yanyin Zhang,†[b] Qingran Yang,[a] Yujun Song *[b] and Yanfeng Gao *[a]

The rapid, accurate, and portable detection of biomarkers plays a central role in clinical diagnostics, food safety, and environmental monitoring. However, conventional molecular diagnostic techniques are often limited by bulky instrumentation, labor-intensive protocols, and complex manipulation. The integration of the CRISPR–Cas system with microfluidics offers a novel diagnostic strategy to overcome these challenges, leveraging the remarkable specificity and sensitivity of CRISPR–Cas along with the miniaturization, integration, high-throughput, and automation of microfluidics. This review aims at summarizing the recent development of microfluidics-integrated CRISPR–Cas systems for biomarker detection, with a specific focus on the advances made over the past five years. Following a snapshot of the working mechanism of the CRISPR–Cas system in diagnostics and the diverse microfluidic setups, we comprehensively overview the applications of this technique for the detection of various biomarkers. Finally, persisting challenges and future trends are critically discussed. Overall, this review demonstrates the potential of microfluidics-integrated CRISPR–Cas systems in facilitating truly rapid, sample-to-answer point-of-care diagnostics, which are essential for global disease surveillance and accessible healthcare.

Received 30th September 2025,
Accepted 23rd October 2025

DOI: 10.1039/d5sd00176e

rsc.li/sensors

Open Access Article. Published on 28 2025. Downloaded on 02.12.2025 02:59:53.
This article is licensed under a Creative Commons Attribution 3.0 Unported Licence.

1. Introduction

The accurate and rapid detection of specific biomarkers is a critical requirement across numerous fields, such as clinical diagnostics, food safety, and environmental monitoring.[1–3] The ideal diagnostic platform should be portable, cost-effective, and capable of delivering a rapid, "sample-to-answer" result without the need for a centralized laboratory.[4] Traditional molecular diagnostic techniques, such as polymerase chain reaction (PCR) and next-generation sequencing (NGS), while highly sensitive, often fall short of these criteria because of their reliance on complex instrumentation and multi-step protocols.[5–7] In recent years, clustered regularly interspaced short palindromic repeats (CRISPR)–CRISPR-associated protein (Cas) technology has revolutionized this landscape.[8] Originally discovered as an adaptive immune system in bacteria and archaea,[9] the CRISPR–Cas technology has been repurposed from its gene-editing origins into a powerful tool for nucleic acid detection owing to the programmable nature and the *trans*-cleavage capability of the system.[10,11] This novel technology has shown excellent performance during recent global health crises, such as the coronavirus disease 2019 (COVID-19) pandemic,[12,13] where the need for rapid, decentralized, and accurate testing has been paramount. This demonstration of real-world utility has underscored the potential of CRISPR for addressing future public health emergencies and democratizing access to molecular diagnostics.[14]

Despite its transformative potential, the widespread application of CRISPR–Cas has been limited by several key practical constraints. For example, to achieve high sensitivity, this technology often requires a pre-amplification step, such as recombinase polymerase amplification (RPA) or loop-mediated isothermal amplification (LAMP).[15] These steps, along with sample preparation and the final detection reaction, are often performed manually in separate vessels, resulting in operational complexity, risk of contamination, and longer detection times. Additionally, the requirement for large quantities of specific samples and reagents can be a limiting factor, particularly for point-of-care (POC) applications where cost and resource efficiency are paramount.[16,17]

This is where microfluidics, the science of controlling fluids on the microscale, offers a compelling solution.[18–20] Capable of efficiently manipulating small volumes of fluids, microfluidics significantly reduces the consumption of

[a] School of Medical Imaging, Wannan Medical College, Wuhu 241002, China. E-mail: gaoyanfeng@wnmc.edu.cn
[b] College of Engineering and Applied Sciences, State Key Laboratory of Analytical Chemistry for Life Science, Nanjing University, Nanjing 210023, China. E-mail: ysong@nju.edu.cn
† These authors contributed equally to this work.

© 2025 The Author(s). Published by the Royal Society of Chemistry

Open Access Article. Published on 28 2025. Downloaded on 02.12.2025 02:59:53.
This article is licensed under a Creative Commons Attribution 3.0 Unported Licence.

samples and expensive reagents, making it highly resource efficient. Furthermore, microfluidic devices, often referred to as "lab-on-a-chip", can integrate multiple laboratory functions into a single miniaturized chip, such as sample purification, mixing, amplification, and detection,[21–23] which facilitates the fabrication of a fully automated and portable "sample-to-answer" workflow, eliminating manual, time-consuming multi-step procedures that are prone to error and contamination.[24,25] Moreover, recent advancements in nanotechnology and nanomaterials for biomedical applications[26–29] has enabled the integration of functional nanomaterials into these chips, which allows for signal amplification without the need for complex pre-amplification steps, and further simplifies the diagnostic process.[30,31] Thus, microfluidic devices capable of automating the entire workflow with minimal reagent requirements, reduced detection time, simplified manipulation, and enhanced detection accuracy, provide a promising way to address the current limitations of CRISPR-based diagnostics.[32]

Therefore, the integration of CRISPR–Cas systems with microfluidics is pioneering a new generation of diagnostic tools, combining the advantages of both techniques, including the high specificity and sensitivity of CRISPR–Cas, as well as the integration, automation, portability, low cost, and rapid detection of microfluidics, which represents a significant leap toward democratizing molecular diagnostics.[33,34] This review delves into the rapid evolution of microfluidics-integrated CRISPR–Cas systems for biomarker detection, focusing on advances over the past five years (from 2020 to 2025). We begin by elucidating the fundamental mechanisms of CRISPR–Cas in diagnostics, and then critically examine the diverse microfluidic strategies enabling its on-chip integration. Subsequently, we showcase the transformative applications of these integrated platforms across various diagnostic fields, and conclude with a forward-looking discussion on the prevailing challenges and future trajectories (Fig. 1).

2. Principle of the CRISPR–Cas system for diagnostics

The CRISPR–Cas system is a powerful and versatile technology that has revolutionized molecular biology and is being applied in a wide range of fields, from gene editing to

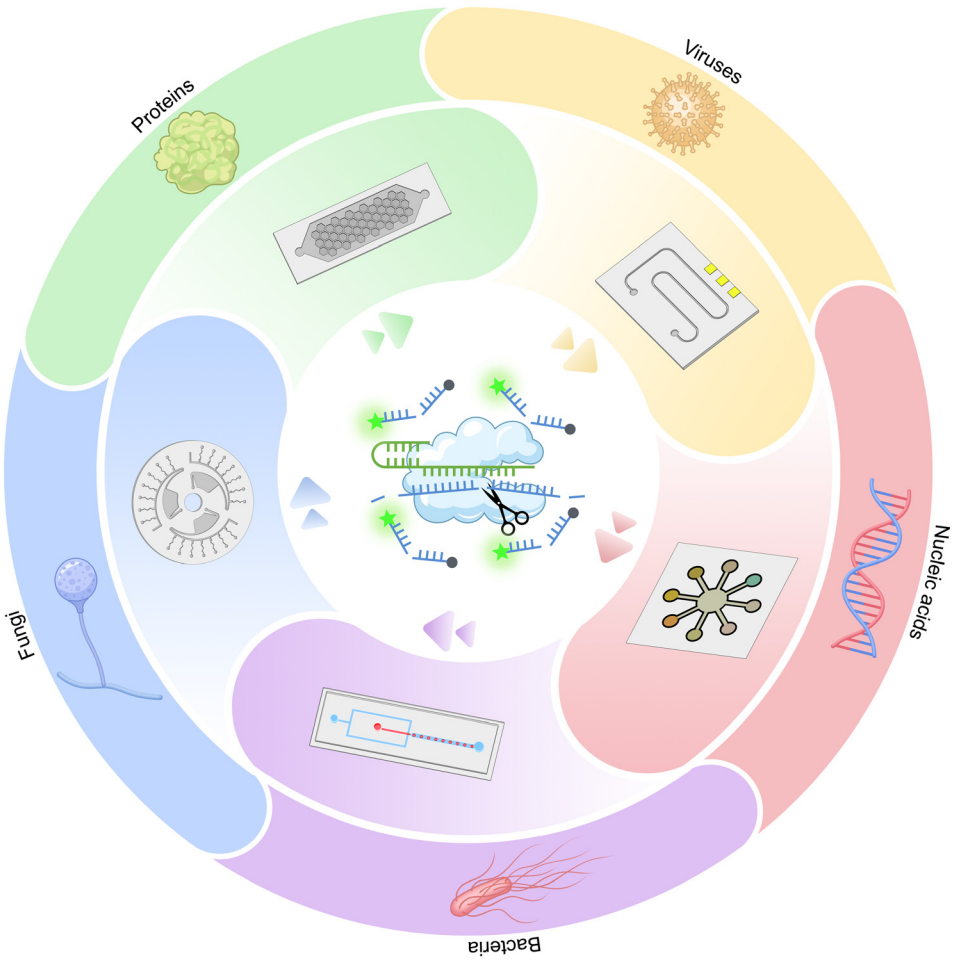

Fig. 1 Schematic illustration of the integration of various microfluidic devices with the CRISPR–Cas system for the detection of diverse biomarkers.

© 2025 The Author(s). Published by the Royal Society of Chemistry

Open Access Article. Published on 28 2025. Downloaded on 02.12.2025 02:59:53.
This article is licensed under a Creative Commons Attribution 3.0 Unported Licence.

Table 1 Comparison of different Cas proteins for nucleic acid cleavage

	Cas9	Cas12	Cas13	Cas14
Primary target	dsDNA	dsDNA	ssRNA	ssDNA
gRNA	crRNA-tracrRNA conjugates	crRNA only	crRNA only	crRNA only
Cleavage pattern	Blunt ends	Sticky ends	Degraded RNA	Degraded DNA
PAM/PFS requirement	PAM: NGG (N: any nucleotide base)	PAM: TTTV (V = A/C/G)	PFS: non-G base preference	Non strict PAM; some require T-rich motifs
Collateral cleavage activity	None	Yes, non-specific cleavage of ssDNA	Yes, non-specific cleavage of ssRNA	Yes, non-specific cleavage of ssDNA
Relative size	~1300–1400 amino acids	~1200–1500 amino acids	~1100–1300 amino acids	~400–700 amino acids
Primary applications	Genome engineering	Biosensing	RNA detection	Ultra-sensitive DNA detection

diagnostics.[35,36] At its core, it is a natural adaptive immune system found in bacteria and archaea to combat invading viruses (bacteriophages) and foreign genetic elements.[37] The system consists of two key components: the CRISPR array and Cas proteins. The CRISPR array is a section of the bacterial genome composed of repeating DNA sequences interspersed with short fragments of DNA, known as "spacers", which are captured from previous viral infections. CRISPR can therefore be regarded as a genetic "memory bank" of foreign invaders. Cas proteins are a diverse family of enzymes that act as workhorses and carry out different functions of the CRISPR system, from acquiring foreign DNA to cleaving it.[38]

Specifically, the system's immune response occurs in three stages. In the adaptation stage, when a bacterium is infected by a virus, some Cas proteins (typically Cas1 and Cas2) capture a small piece of viral DNA adjacent to the protospacer adjacent motif (PAM) and integrate it into its own CRISPR array as a new spacer. Next, in the expression stage, the CRISPR array, including the spacer sequences, is transcribed into a long RNA molecule and processed into short CRISPR RNAs (crRNAs), each containing a single spacer sequence. Finally, in the interference stage, when the virus invades again, the crRNA, guided by the spacer, recognizes and binds to the viral nucleic acids. Another Cas protein (such as Cas9, Cas12, or Cas14) is then activated, forming a complex with the crRNA (or crRNA conjugated with a tracrRNA molecule for Cas9) and serving as "molecular scissors" to precisely cleave the foreign nucleic acids with a specific PAM. Note that Cas13 targets a single-stranded RNA (ssRNA) rather than DNA, and recognizes target RNA according to the protospacer flanking site (PFS) but not PAM. By eliminating viral nucleic acid, the bacterium successfully defends itself from the invading virus.[39,40] It should be highlighted that different Cas proteins exhibit different activating and cleaving

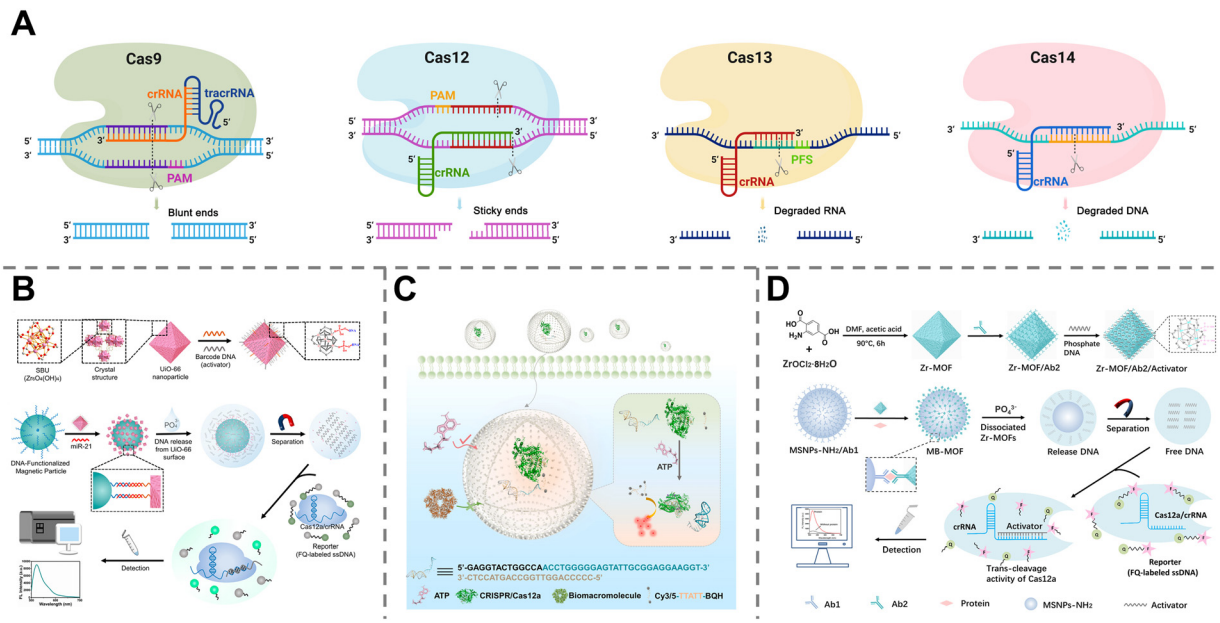

Fig. 2 CRISPR–Cas systems for diagnostics. (A) Cleavage mechanisms of different Cas proteins. (B) Nucleic acid detection on the basis of the *trans*-cleavage activity of the Cas proteins. Reprinted with permission from ref. 43. Copyright 2022 American Chemical Society. (C) An aptamer-based strategy to detect intracellular ATP. Reprinted with permission from ref. 48. Copyright 2022 Elsevier. (D) Signal conversion based on a MOF nanoparticle allowing for protein detection. Reprinted with permission from ref. 49. Copyright 2023 American Chemical Society.

Open Access Article. Published on 28 2025. Downloaded on 02.12.2025 02:59:53.
This article is licensed under a Creative Commons Attribution 3.0 Unported Licence.

mechanisms, resulting in various biomedical applications (Table 1 and Fig. 2A).

Recently, scientists have repurposed the CRISPR–Cas system as a powerful diagnostic tool by maintaining its core function of nucleic acid cleavage.[41,42] In short, ssRNA containing a sequence complementary to the target nucleic acid (DNA or RNA), known as guide RNA (gRNA), is artificially engineered to serve the same targeting function as the crRNA (or crRNA–tracrRNA conjugates) in the natural bacterial system. When the gRNA binds to its target, the Cas protein undergoes a conformational change that directs it to cut the target nucleic acid. It should be highlighted that some Cas proteins (typically Cas12, Cas13 and Cas14) exhibit a remarkable "collateral cleavage" activity, *i.e.*, the capability to indiscriminately cleave any nearby nucleic acid molecules, which offers the possibility to generate a detectable signal rather than simply cleaving the target.

One of the most common signal conversion methods is fluorescence, where a reporter molecule composed of a short nucleic acid with a fluorescent dye on one end and a quencher on the other, is added to the system. In its intact state, the quencher sits next to the dye, preventing it from emitting a signal. When the Cas protein is activated, it collaterally cleaves the reporter molecule and separates the dye and the quencher, thus releasing measurable fluorescence signals (Fig. 2B).[43] Alternatively, for visual simplicity, colorimetric signals can be used on the basis of reporters linked to colored particles (such as gold nanoparticles) that result in a visible color change upon cleavage.[44,45] Additionally, electrochemical methods have been developed for quantitative detection, where the cleavage of a reporter probe changes the electrical properties of the solution, which can then be measured by a portable potentiostat.[46,47] These signal conversion strategies successfully translate the molecular *trans*-cleavage event into a user-friendly and quantifiable output, making the assay adaptable to different POC settings.

While the core function of the CRISPR–Cas system is nucleic acid cleavage, its diagnostic utility has been expanded far beyond nucleic acid detection through reasonable engineering of detection systems. The key principle is to convert the quantification of the target non-nucleic acid biomarker to a downstream CRISPR–Cas reaction. For example, our group has proposed an aptamer-based strategy to detect ATP, a small-molecule nucleotide. Initially, the ATP aptamer was hybridized with the activator strand of the CRISPR–Cas system, and encapsulated in a hollow COF to facilitate delivery into cells. Upon encountering ATP, the aptamer captures ATP and releases the DNA activator, which triggers the *trans*-cleavage activity of the Cas12a protein. Cas12a cleaved the quenched DNA reporter in the system and restored the fluorescence signal, resulting in the quantitative detection of intracellular ATP (Fig. 2C).[48] Another work of our group reported zirconium-based metal–organic framework (MOF) nanoparticles co-functionalized with activators and detection antibodies of the target protein, which could be immobilized onto capture antibody-functionalized magnetic nanoparticles in the presence of the target protein through antibody–antigen affinity, leading to the conversion of protein quantity to activator number. Upon magnetic separation and MOF dissociation, the activators are released to initiate the CRISPR–Cas reaction, achieving sensitive detection of protein biomarkers (Fig. 2D).[49]

In brief, being capable of detecting a single nucleic acid sequence with unparalleled accuracy by precise design of the gRNA, the CRISPR–Cas system has the core advantages of high specificity and programmability. In addition, through collateral cleavage activity, the system also offers a powerful, built-in signal conversion and amplification mechanism, leading to extremely high sensitivity. Nevertheless, practical challenges, such as the multi-step detection process, the lack of integration and the risk of cross-contamination, should be addressed before the widespread use of the CRISPR–Cas system for POC applications.

3. Microfluidic devices for integrated CRISPR–Cas systems

While the CRISPR–Cas system provides unparalleled specificity for biomarker detection, its manual, multi-step processes, which involve mainly separate processes for sample preparation, pre-amplification, and detection, present significant hurdles for widespread, decentralized use. Microfluidics, being capable of precisely controlling fluids at the microscale, can effectively create a closed system, integrate multiple functions, and minimize handling steps, which directly addresses these limitations and offers the possibility to automate the entire "sample-to-answer" workflow.[50] In this section, we delve into the microfluidic devices most commonly employed with CRISPR–Cas systems, mainly including centrifugal microfluidic devices, microdroplets, microfluidic array chips, microfluidic paper-based analytical devices, and electrochemical microfluidic devices (Table 2).

3.1. Centrifugal microfluidic devices

Centrifugal microfluidics, also known as "lab-on-a-disc", uses a motor to spin a disc containing microfluidic channels and chambers, causing fluids to move outwards from the center *via* centrifugal force.[51] By precisely varying the rotational speed and direction, different processes, such as pumping, mixing, and separation, can be controlled and automated.[52] This high versatility makes it possible to integrate multi-step diagnostic workflows into a single device, from sample preparation, such as cell separation and nucleic acid extraction, to downstream amplification and detection.[53,54] By consolidating multiple manual steps, centrifugal microfluidics significantly reduces hands-on time and the risk of contamination, paving the way for automated and user-friendly testing in diverse settings and demonstrating wide applications for rapid and sensitive diagnostics.

© 2025 The Author(s). Published by the Royal Society of Chemistry

Open Access Article. Published on 28 2025. Downloaded on 02.12.2025 02:59:53.
This article is licensed under a Creative Commons Attribution 3.0 Unported Licence.

Table 2 Common microfluidic devices for integration with the CRISPR–Cas system and their characteristics

Microfluidic device	Key features	Advantages	Disadvantages	Functions in diagnostics
Centrifugal microfluidic devices	Use centrifugal force (spinning motor) to control fluid movement (pumping, mixing, separation)	High versatility and automation level	Requirement of a motor/spinner to drive the disc	Sample preparation
		Significant reduction in hands-on time	High complexity, volume, and cost	Multi-step workflow automation
		Strong capability for complex sample preparation	Less portable for certain POC applications	Compatible with isothermal amplification
Microdroplets	Encapsulate reactions in tiny, discrete aqueous droplets within an immiscible fluid, acting as self-contained microreactors	Extremely high throughput	Complex instrumentation for droplet generation	Target separation and isolation
		Single-molecule resolution Multiplexing capability Minimal reagent consumption Reduced assay time	Less available for low-cost POC applications	Parallel reactions
Microfluidic array chips	Arrange fundamental structures, such as wells and chambers, in a patterned format to partition the reaction mixture	High throughput	Difficult to integrate a complex multi-step workflow	Sample partitioning
		Multiplexing capability Reduced consumption of reagents and samples Single-cell/single-molecule sensitivity	Complex manufacturing process	Parallel and simultaneous detection
μPADs	Use porous materials and passive capillary action to guide fluid flow	No need for external pumps or power	Limited ability for complex sample preparation	Workflow integration
		Extremely simple, low-cost, disposable, and highly portable	Challenging to achieve precise quantification	Target detection Straightforward signal readout by the naked eye
Electrochemical devices	Integrate electrodes directly into the chip to convert a reaction into a measurable electrical signal	Simple and portable instrumentation	Potential non-specific adsorption of biomolecules on the electrodes	Potential for amplification-free detection
		Ideal for highly automated, fully integrated POCT Potential for amplification-free and highly sensitive diagnostics	Difficult for highly integrated production	

The integration of a centrifugal microfluidic device with the CRISPR–Cas technique facilitates the automation of complex, multi-step experimental workflows. For example, a centrifugal microfluidic platform was developed for automated, rapid, and sensitive bacterial detection on the basis of the RAA-T7-CRISPR–Cas13a assay. The chip contained eight functional chambers and three siphon valves to highly integrate various manipulations, including sample loading, target capture, washing, nucleic acid elution, pre-amplification, *in vitro* transcription, CRISPR–Cas13a reaction, and fluorescence detection. Finally, the detection of Salmonella in chicken supernatants at a limit of detection (LOD) of 10 CFU mL^{-1} has been achieved (Fig. 3A).[55] Centrifugal microfluidics-integrated CRISPR–Cas platforms have also been applied for the detection of other biomarkers, such as Ebola virus,[56] and SARS-CoV-2 virus.[57,58]

Although centrifugal microfluidics offers significant advantages, such as simplified operation, integrated sample preparation, and a high level of automation, the need for a motor or spinner to drive disc movement inherently increases device complexity, volume, and fabrication cost. These challenges must be addressed before the platforms can be adopted for a wider range of POC applications.

3.2. Micordroplets

Microdroplet microfluidics is a technology that leverages an immiscible fluid (such as oil) to encapsulate tiny, discrete aqueous droplets, each acting as a self-contained microreactor. With the optimization of the droplet generation structure, it is possible to form thousands of droplets in a short time, each containing a specific reagent system, allowing for thousands or even millions of parallel reactions

Open Access Article. Published on 28 2025. Downloaded on 02.12.2025 02:59:53.
This article is licensed under a Creative Commons Attribution 3.0 Unported Licence.

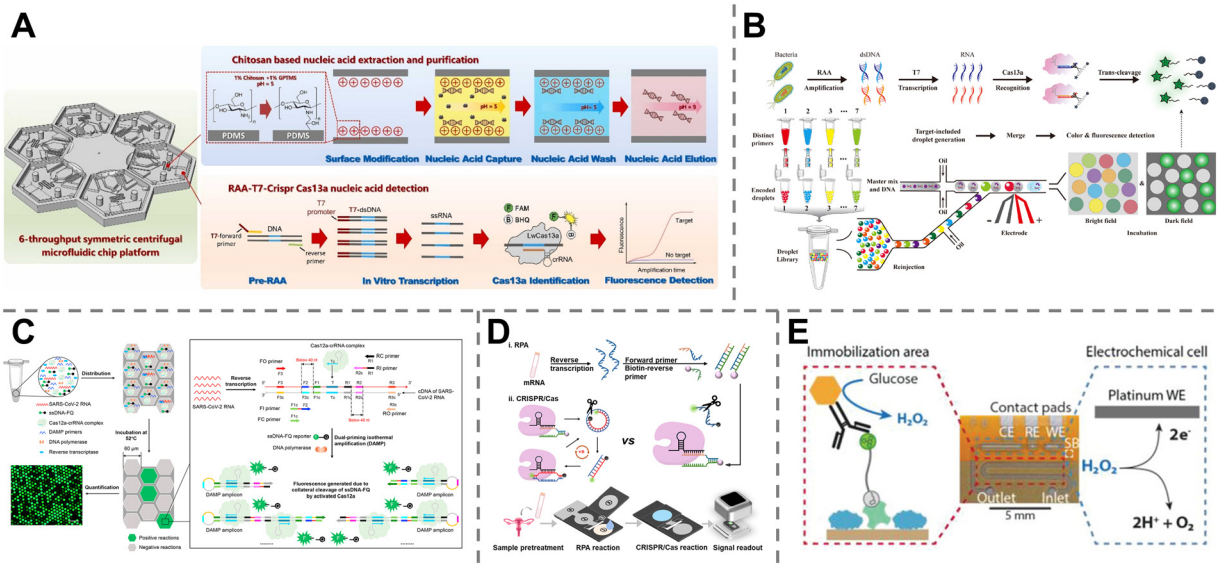

Fig. 3 Diverse microfluidic devices integrated with the CIRSPR–Cas systems for biomarker detection. (A) A fully integrated centrifugal microfluidic chip for the automatic detection of *Salmonella* in chicken supernatants relying on the CRISPR–Cas13a reaction. Reprinted with permission from ref. 55. Copyright 2023 Elsevier. (B) Encoded microfluidic droplets integrated with CRISPR–Cas for simultaneous detection of multiple bacteria. Reprinted with permission from ref. 59. Copyright 2024 Elsevier. (C) A digital microwell chip for the detection of SARS-CoV-2. Reprinted with permission from ref. 60. Copyright 2021 Elsevier. (D) A "sample-to-answer" μPAD for HPV diagnosis. Reprinted with permission from ref. 61. Copyright 2025 American Chemical Society. (E) An electrochemical microfluidic chip for the simultaneous detection of two microRNAs. Reprinted with permission from ref. 62. Copyright 2019 The Authors.

simultaneously, without cross-contamination.[63,64] In addition, typically ranging from picoliters to nanoliters in size, microdroplets enable accelerated reaction kinetics, which dramatically reduces assay time and reagent consumption.[65,66]

When integrated with the CRISPR–Cas system, microdroplets are particularly useful for high-throughput screening and digital assays.[67] For example, by combining droplet microfluidics and the droplet encoding strategy, various foodborne pathogens can be detected simultaneously through a single test, without any cross-contamination. Specifically, each type of bacterial sample was encapsulated into microdroplets encoded with distinct colors. These encoded droplets were randomly mixed together and reinjected into another chip, where each droplet was merged with one-pot CRISPR detection reagents. Finally, the target nucleic acids were detected by Cas13a, and the corresponding fluorescence signals were generated for bacterial quantification. This platform achieved a high-throughput multiplexed assay of 7 bacteria with high specificity and sensitivity in 1 h (Fig. 3B).[59]

Microdroplet microfluidics offers compelling advantages by enabling single-molecule resolution with extremely high throughput and minimal reagent consumption. These capabilities make the technique exceptionally well-suited for absolute quantification and give it immense potential in applications ranging from single-cell analysis to highly sensitive biomarker detection. However, the primary disadvantage lies in the complex instrumentation required for reliable droplet generation and detection, which presents the main challenge to the development of simple, low-cost and POC applications.

3.3. Microfluidic array chips

Microfluidic arrays utilize a patterned arrangement of fundamental structures, such as pillars, wells, and chambers, to efficiently achieve target screening, capture and detection.[68–70] By pre-loading each reaction site with a specific detection probe, a single sample can be screened for numerous targets in one test, which is particularly valuable for multiplexing and high-throughput detection, without cross-contamination.[71,72] In addition, the extremely small volumes within each reaction site, typically ranging from picoliters to nanoliters, drastically reduce the consumption of reagents and samples, lowering overall costs. Microfluidic arrays also allow for absolute quantification of targets with high sensitivity, even at the single-cell or single-molecule level, which makes them an ideal platform for a wide range of diagnostic applications.[73]

Microfluidic arrays can be easily integrated with the CRISPR–Cas system by pre-loading different gRNAs at each individual reaction site, to enable parallel and simultaneous detection of multiple biomarkers in one run. For example, CRISPR–Cas12a-based digital detection of SARS-CoV-2 RNA has been realized by using a microfluidic chip containing over ten thousand sub-nanoliter microwells. The reaction mixture was partitioned into the microwells, incubated to induce the CRISPR reaction, and generated a detectable fluorescence signal. This strategy

© 2025 The Author(s). Published by the Royal Society of Chemistry

Open Access Article. Published on 28 2025. Downloaded on 02.12.2025 02:59:53. This article is licensed under a Creative Commons Attribution 3.0 Unported Licence.

allowed highly sensitive quantification of SARS-CoV-2 with an LOD as low as 5 copies per μL without RNA extraction (Fig. 3C).[60]

Microfluidic arrays significantly enhance the diagnostic capability of CRISPR by providing a high-density, comprehensive diagnosis while maintaining the advantages of miniaturization, reduced reagent consumption, and multiplexing. Notable disadvantages and challenges remain in integrating a complex multi-step workflow into a single microfluidic array chip and the complex manufacturing process, which often limits its scalability.

3.4. Microfluidic paper-based analytical devices

Paper-based microfluidics is a technology that uses porous materials, such as paper or nitrocellulose, as a substrate to guide fluid movement. Microfluidic paper-based analytical devices, called μPADs, are generally fabricated by creating hydrophilic channels and hydrophobic barriers on the substrate, to confine and manipulate fluid flow.[74,75] The core principle of μPADs lies in passive capillary action, which moves the liquid sample without the need for external pumps or power sources. This simplicity makes μPADs low-cost, disposable, and user-friendly, allowing for a rapid, visual readout that is ideal for POC applications, especially in resource-limited zones or at home.[76,77]

When μPADs are combined with the CRISPR–Cas system, it is possible to develop a cost-effective, highly-integrated, and automated diagnostic platform for fast and straightforward biomarker detection. For example, an innovative μPAD integrated with a valve and multiple distinct zones was developed to automate the entire "sample-to-answer" process, *i.e.*, from RPA for nucleic acid amplification and CRISPR detection, to fluorescence signal readout. This fully integrated, low-cost, and portable diagnostic platform has allowed for rapid and highly sensitive screening of high-risk HPV infections, with an LOD of 1 fM within 1 h (Fig. 3D).[61] It is also possible to incorporate other signal output modalities into μPADs. For example, a highly sensitive RPA-Cas12a-μPAD was proposed for the rapid detection of *Salmonella typhimurium (S. typhimurium)* in food, achieving an ultralow LOD of 3–4 CFU mL^{-1} within 45 min by translating Cas12a *trans*-cleavage activity into a supersensitive surface-enhanced Raman scattering (SERS) signal readout.[78]

Although μPADs possess the distinct benefits of ultra-low cost, straightforward fabrication, inherent portability, and simplified result output, their utility is significantly constrained by the difficulty of incorporating complex sample preparation steps and the challenge of reliable quantitative analysis.

3.5. Electrochemical microfluidic devices

Electrochemical microfluidic chips represent another distinct diagnostic platform developed by integrating an electrochemical sensing system into the chip, and are designed to convert a molecular recognition event into a measurable electrical signal.[79] The key advantage lies in bypassing the need for bulky and expensive signal readout devices, such as fluorescence scanners or spectrophotometers used in traditional optical detection methods.[80,81] This simple, portable instrumentation makes electrochemical microfluidic chips ideal candidates for developing highly automated, fully integrated, and highly sensitive diagnostic tools in resource-limited settings.[82]

A traditional electrochemical sensing system generally works based on three electrodes:[83] a working electrode, a reference electrode, and a counter electrode. The working electrode is where the CRISPR reaction takes place to generate the current signal. The reference electrode provides a stable, known, and unchanging potential against which the potential of the working electrode is measured. The counter electrode, also called the auxiliary electrode, completes and manages the current flow in the circuit to ensure that all the current generated at the working electrode can be matched, and that the reference electrode is protected from high current flow.[84] For example, a microfluidic chip equipped with a three-electrode electrochemical cell (platinum working electrode, silver/silver chloride reference electrode, and platinum counter electrode) was developed and used along with the CRISPR–Cas13a technique, for miRNA detection. Following the off-chip recognition of miRNA by Cas13a proteins, the mixture was injected into the immobilization area of the microfluidic chip, where the noncleaved reporter RNA was captured and linked to glucose oxidase (GOx). GOx catalyzed the introduced glucose and produced H_2O_2, which was amperometrically detected by the working electrode. This amplification-free setup detected the tumor-related biomarkers miR-19b and miR-20a with an LOD of 10 pM (Fig. 3E).[62] Other electrochemical modules, such as organic electrochemical transistors, have also emerged to support the CRISPR–Cas reaction for diagnostic applications.[85]

By enabling highly sensitive, amplification-free, and rapid diagnostics through miniaturized chips without the use of other signal transduction and output devices, electrochemical microfluidic biosensors show great advantages in the development of point-of-care testing (POCT) tools. However, the potential non-specific adsorption of biomolecules on the electrode can interfere with the detection accuracy. Challenges also lie in the mass production of integrated, complex microfluidic chips at low cost while maintaining high uniformity and stability.

3.6. Other microfluidic devices

In addition to the most commonly employed microfluidic platforms described above, innovative architectures continue to emerge, integrating with the CRISPR–Cas technology to meet the demand for simplified operation, enhanced visualization, and portability in low-cost, user-friendly diagnostics. Among these, SlipChip and volumetric bar-chart chip (V-Chip) deserve particular attention.

A SlipChip is usually composed of two plates precisely patterned with microchambers and channels, which controls

Open Access Article. Published on 28 2025. Downloaded on 02.12.2025 02:59:53.
This article is licensed under a Creative Commons Attribution 3.0 Unported Licence.

fluid manipulations, such as mixing, separation, and compartmentalization through relative sliding between plates.[86] This simple movement without complex pumps or valves offers significant advantages, including simplicity, portability, multiplexing, high-throughput, low reagent consumption, *etc.*, and shows promising application in nucleic acid quantification when combined with CRISPR–Cas systems.[87] However, complex chip fabrication and difficulty in precise sealing remain the key challenges that should be overcome. The V-Chip is a novel type of gas-propelled biosensor that converts the concentration of a target analyte into a proportional volume of gas which further pushes the movement of ink bar along the microchannel, resulting in a readable result with the naked eye.[88] In addition, by designing multiple parallel channels, it is possible to achieve simultaneous detection of different analytes in one assay. The V-Chip usually serves to support multiplex assays and signal readout in CRISPR-based sensing applications.[89,90] This platform, which does not require complex instruments, is low cost and highly portable, making it ideal for POCT and low-resource settings. However, this simplicity comes at the cost of potential readout inaccuracies and sensitivity to environmental changes. Moreover, conventional syringe-driven microfluidic devices also remain indispensable for continuous-flow CRISPR studies.[91]

These creative microfluidic strategies underscore the remarkable adaptability of microfluidic design for CRISPR diagnostics, offering advantages in simplicity, cost, and user accessibility, while addressing different challenges in manipulation and readout. Continued integration of these designs with portable signal transduction and low-cost manufacturing techniques will further advance the development of accessible, fully instrument-free, and deployable diagnostic tools for a wide range of real-world applications.

4. Microfluidics-integrated CRISPR–Cas system for biomarker detection

The integration of the CRISPR–Cas system with microfluidics creates a powerful new diagnostic platform, by combining the advantages of both components, including the remarkable specificity and sensitivity of the CRISPR–Cas system and the ability to create fast, practical, integrated laboratory tools of the microfluidic technique. This section explores the wide range of applications of microfluidics-integrated CRISPR–Cas systems in the detection of disease biomarkers (Table 3), including nucleic acids, viruses, bacteria, mycotoxins, *etc.*, with a special emphasis on their ability for simultaneous detection of multiple targets, and "all-in-one" diagnostic tools.

4.1. Nucleic acids

Nucleic acid detection is a cornerstone of modern molecular diagnostics, widely applied in the diagnosis of infectious diseases, genetic disorders, and cancer.[92–94] Although traditional methods, such as PCR, offer high sensitivity and are regarded as the gold standard, their further advancement is still limited, mainly due to the requirement of bulky thermal cyclers, complex manual handling steps for nucleic acid extraction and amplification, and the high risk of cross-contamination. The integration of microfluidics with CRISPR–Cas systems effectively addresses these limitations. On the one hand, CRISPR–Cas provides exceptional specificity through targeted cleavage and robust signal amplification, guaranteeing the sensitivity and accuracy of detection. On the other hand, the microfluidic platform, with its high level of integration, streamlines and automates complex, multi-step operations, not only making the assay remarkably fast and efficient but also avoiding cross-contamination.

The microfluidics-integrated CRISPR–Cas system allows highly sensitive and specific nucleic acid detection with a reduced detection time. For example, by combining CRISPR–Cas12a and multiplex RPA in a microfluidic chip with a central well and 30 spoke microchannels, a simple 30-plexed starburst-shaped chip was designed to simultaneously test up to 30 nucleic acid targets through microfluidic space coding. The LOD was 0.26 attomole, and the device efficiently detected nine HPV subtypes in clinical samples with a sensitivity of 97.8% and specificity of 98.1% (Fig. 4A).[95] In addition, this technique also offers the possibility of eliminating the pre-amplification round while maintaining the detection accuracy. A negative pressure-driven droplet microfluidic chip was fabricated to generate monodisperse droplets containing the Cas13a system, crRNA, and the target RNA sample. The CRISPR reactions within the droplets released fluorescent tags, causing the droplet to emit a green fluorescence signal, which was observed and analysed under an inverted fluorescence microscope. Without any pre-amplification process, this simple setup successfully detected SARS-CoV-2 RNA from human saliva samples with an LOD as low as 470 aM within only 30 min (Fig. 4B).[96] Another microfluidic biosensor focusing on the CRISPR–Cas13a-powered electrochemical readout has also been reported to realize simultaneous detection of two common microRNAs, miRNA-19b and miRNA-20a, without any pre-amplification process.[97]

Additionally, microfluidics-integrated CRISPR–Cas systems allow for the integration of complex assay processes, such as sample preparation, reaction, and signal readout, into a single chip, thus drastically reducing the detection time. For example, a three-layered stand-alone microfluidic device made of poly(methyl methacrylate) (PMMA) sheets was fabricated to carry out nucleic acid detection through a three-step on-chip assay, consisting of RPA for isothermal DNA amplification, CRISPR cleavage for fluorescence signal generation, and visual signal readout *via* a lateral flow dipstick (LFD). Note that the chip was adhered to a heating membrane to ensure the working temperature. The system

© 2025 The Author(s). Published by the Royal Society of Chemistry

Open Access Article. Published on 28 2025. Downloaded on 02.12.2025 02:59:53.
This article is licensed under a Creative Commons Attribution 3.0 Unported Licence.

Table 3 Microfluidics-integrated CRISPR–Cas systems for diverse biomarker detection

Microfluidic device	Cas protein	Target biomarker	LOD	Detection time	Application context	References
Centrifugal microfluidic platform	Cas13a	*Salmonella*	10 CFU mL^{-1}	1 h	Bacterial detection	55
Centrifugal microfluidic device	Cas12a	7 viruses	N.A.	30 min	Virus detection	56
Centrifugal microfluidic device	Cas12a	SARS-CoV-2 viruses	1 copy per μL	30 min	COVID-19 diagnosis	57
Centrifugal microfluidic device	Cas12a	12 respiratory viruses	2 copies per μL	30 min	Infectious disease diagnosis	58
Encoded microdroplets	Cas13a	7 foodborne bacteria	10 copies per μL	1 h	Multiplex bacterial detection	59
Microfluidic array chip	Cas12a	SARS-CoV-2 RNA	5 copies per μL	N.A.	COVID-19 diagnosis	60
μPAD	Cas12a	HPV E7 gene	1 fM	1 h	HPV diagnosis	61
Electrochemical microfluidic chip	Cas13a	miR-19b and miR-20a	10 pM	4 h	Brain cancer diagnosis	62
μPAD	Cas12a	*S. typhimurium*	3–4 CFU mL^{-1}	45 min	Food pathogen detection	78
Electrochemical microfluidic device	Cas12a	*S. aureus* 6S dsDNA, SARS-CoV-2 N gene, and EGFR L858R mutations	8.1×10^{-17} M, 7.6×10^{-17} M and 1.0×10^{-16} M	55 min	Nucleic acid detection	85
Starburst-shaped chip	Cas12a	HPV subtype DNA	0.26 aM	40 min	HPV diagnosis	95
Negative pressure-driven droplet chip	Cas13a	SARS-CoV-2 RNA	470 aM	30 min	COVID-19 diagnosis	96
Electrochemical microfluidic biosensor	Cas13a	miRNA-19b and miRNA-20a	2–18 pM	N.A.	MicroRNA detection	97
Three-layered PMMA microfluidic chip	Cas12a	HPV16 and HPV18 DNA	0.5 nM and 1 aM	30 min	HPV diagnosis	98
Multi-step SlipChip	Cas12a	SARS-CoV-2 RNA	400 copies per mL	60 min	COVID-19 diagnosis	99
Microdroplet biosensor	Cas12a	Meat genomic DNA	10 copies per μL	60 min	Food authenticity	100
Centrifugal microfluidic chip	Cas12a	SARS-CoV-2 RNA	1 copy per μL	50 min	COVID-19 diagnosis	101
Portable centrifugal microfluidic system	Cas13a	10 virus RNA	1 copy per reaction	45 min	Virus multiplexing	102
Self-contained microfluidic chip	Cas12a	SARS-CoV-2 RNA	100 copies per test	N.A.	COVID-19 diagnosis	103
Centrifugal microfluidic chip	Cas12a	SARS-CoV-2 RNA	250 copies per mL	30 min	COVID-19 diagnosis	104
Microfluidic array chip	Cas12a	SARS-CoV-2 variants, influenza A/B, HRSV	100 copies per mL	60 min	Virus multiplexing	105
Microfluidic dual-droplet device	Cas12a	HPV 16 and HPV 18	0.018 nM and 0.025 nM	<30 min	HPV diagnosis	106
Stand-alone SlipChip	Cas12a	HPV16 and HPV18	6 copies per reaction	36 min	HPV diagnosis	107
Pneumatic microfluidic chip	Cas13a	Ebola virus	20 PFU mL^{-1}	5 min	Ebola virus detection	108
Centrifugal microfluidic chip	Cas14a	Four geminiviruses	10 fM	5 min	Agricultural diagnosis	109
Digital microfluidic chip	Cas12a	*Staphylococcus aureus*	32 CFU mL^{-1}	55 min	Bacterial detection	110
Microwell array-based digital chip	Cas12a	Viable *E. coli* O157:H7	36 CFU mL^{-1}	15 min	Viable bacterial differentiation	111
Finger-actuated pneumatic microfluidic chip	Cas12a	7 foodborne bacteria	500 CFU mL^{-1}	60 min	Multiplex bacterial detection	112
Centrifugal microfluidic chip	Cas13a	12 respiratory bacteria	10 CFU mL^{-1}	40 min	Multiplex bacterial detection	113
μPAD	Cas12a	Candida and aspergillus	4.90 and 4.13 CFU mL^{-1}	N.A.	Fungi detection	114
Electrochemical centrifugal chip	Cas12a	Ochratoxin A	1.21 pg mL^{-1}	N.A.	Mycotoxin detection	115
Microfluidic multi-chamber chip	Cas12a	6 mycotoxins	1.4 to 3.9 fg mL^{-1}	40 min	Mycotoxin multiplexing	116

Open Access Article. Published on 28 2025. Downloaded on 02.12.2025 02:59:53.
This article is licensed under a Creative Commons Attribution 3.0 Unported Licence.

Table 3 *(continued)*

Microfluidic device	Cas protein	Target biomarker	LOD	Detection time	Application context	References
Temperature-programmed centrifugal chip	Cas12a	*Treponema pallidum*	10 copies per μL	30 min	Syphilis diagnostics	117

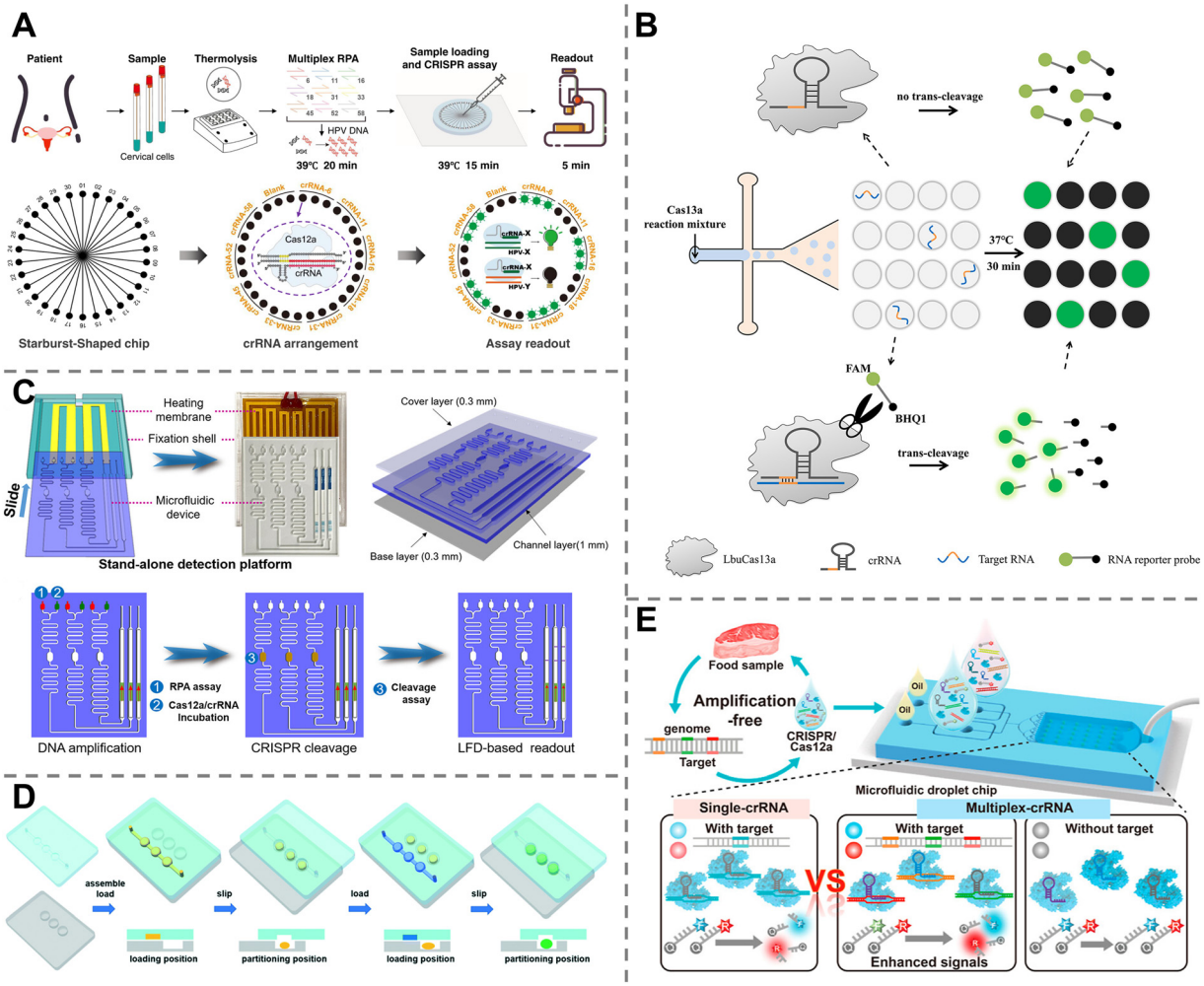

Fig. 4 Microfluidic CRISPR–Cas system for nucleic acid detection. (A) A radially arranged microfluidic chip combined with CRISPR–Cas12a and RPA for highly sensitive detection of nine HPV subtypes in clinical samples. Reprinted with permission from ref. 95. Copyright 2022 Springer Nature. (B) A negative pressure-driven droplet microfluidic chip for SARS-CoV-2 RNA detection in human saliva samples. Reprinted with permission from ref. 96. Copyright 2023 American Chemical Society. (C) A three-layered stand-alone microfluidic device for HPV16 and HPV18 detection through a three-step on-chip assay. Reprinted with permission from ref. 98. Copyright 2023 American Chemical Society. (D) A two-step SlipChip incorporating a multi-step workflow for the automatic detection of SARS-CoV-2 nucleic acid. Reprinted with permission from ref. 99. Copyright 2022 Royal Society of Chemistry. (E) A CRISPR–Cas12a-integrated biosensor based on microdroplets for digital single-molecule DNA detection. Reprinted with permission from ref. 100. Copyright 2024 American Chemical Society.

achieved highly sensitive detection of human papillomavirus (HPV) subtypes, specifically HPV16 and HPV18, from clinical human cervical cell samples, with LODs as low as 0.5 nM and 1 aM, for unamplified and amplified plasmids, respectively, within 30 min (Fig. 4C).[98] A two-step SlipChip was also implemented to incorporate a multi-step process, including sample division, assay manipulation and signal readout, into a single chip for the automatic detection of SARS-CoV-2 nucleic acid. The sample was first loaded and partitioned into 2400 well-arranged droplets of 3.2 nL within the meticulously designed "chain-of-pearl" channels, where the digital loop-mediated isothermal amplification (dLAMP) reaction was initiated to amplify the target nucleic acids. A simple slipping operation was subsequently performed to deliver the Cas12a protein and crRNA into the droplets, inducing the CRISPR reaction to generate fluorescence signals, which were further measured to quantify the target concentration. This design significantly simplified the

© 2025 The Author(s). Published by the Royal Society of Chemistry

Open Access Article. Published on 28 2025. Downloaded on 02.12.2025 02:59:53.
This article is licensed under a Creative Commons Attribution 3.0 Unported Licence.

manipulation of the multi-step assay, and the total processing time was approximately 60 min (Fig. 4D).[99]

Furthermore, by leveraging smartphone interfaces and their integrated data processing, microfluidics-integrated CRISPR–Cas systems can achieve a true "sample-to-answer" workflow.[85] A CRISPR–Cas12a-integrated biosensor based on microdroplets has been developed to realize digital single-molecule DNA detection without pre-amplification. Genomic DNA was extracted, mixed with CRISPR–Cas12a-crRNA assay buffer, and injected into the microfluidic chip to generate picoliter-sized water-in-oil microdroplets. In the presence of the target gene, the Cas12a enzyme is activated and cleaves the fluorescent reporters, resulting in the emission of the fluorescence signal within the microdroplets. These fluorescent microdroplets were then counted *via* a custom-built smartphone application to quantify target DNA for meat species authenticity. The biosensor achieved an extremely low LOD, down to 10 copies per μL, with a linear range from 10

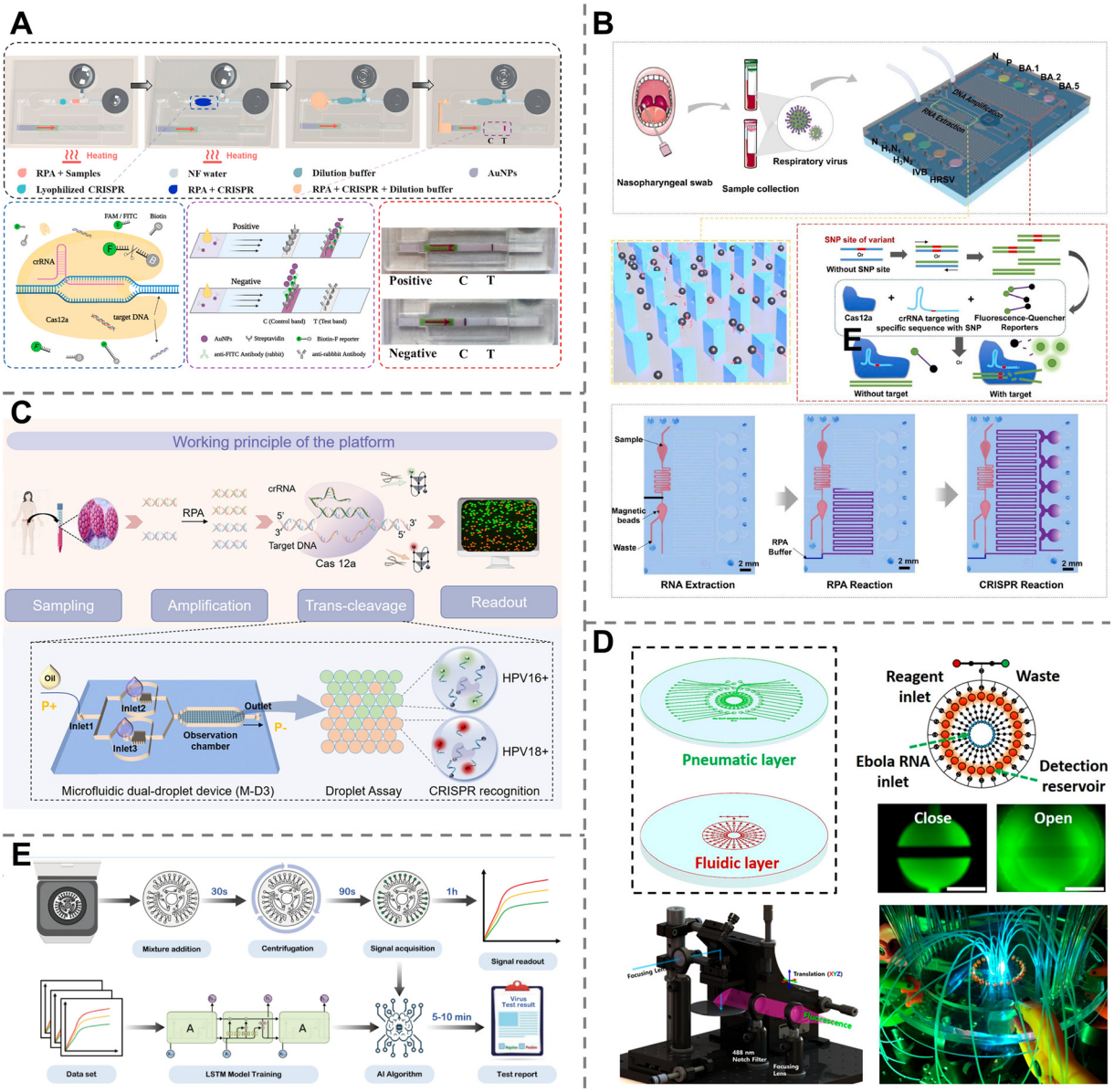

Fig. 5 Microfluidic CRISPR–Cas system for virus detection. (A) A self-contained microfluidic chip integrating a multi-step workflow for SARS-CoV-2 detection. Reprinted with permission from ref. 103. Copyright 2022 Elsevier. (B) A highly integrated, fully enclosed lab-on-a-chip CRISPR system for SARS-CoV-2 variant differentiation. Reprinted with permission from ref. 105. Copyright 2023 Elsevier. (C) A microfluidic dual-droplet device driven by pressure and vacuum for simultaneous detection of HPV nucleic acid targets. Reprinted with permission from ref. 106. Copyright 2023 American Chemical Society. (D) A pneumatic microfluidic chip containing 24 parallel reaction structures for the automatic detection of Ebola virus. Reprinted with permission from ref. 108. Copyright 2019 American Chemical Society. (E) A portable centrifugal microfluidic chip integrated with AI for the detection of multiple devastating geminiviruses in tomato plants and whitefly vectors. Reprinted with permission from ref. 109. Copyright 2025 Elsevier.

Open Access Article. Published on 28 2025. Downloaded on 02.12.2025 02:59:53. This article is licensed under a Creative Commons Attribution 3.0 Unported Licence.

to 10 000 copies per μL, within 60 min (Fig. 4E).[100] Such fully integrated sample-to-answer devices have also been reported for ultra-sensitive detection of nucleic acids from SARS-CoV-2 (ref. 101) and other viruses.[102]

Taken together, by combining the remarkable specificity of CRISPR–Cas with the automation and miniaturization of microfluidics, the microfluidics-integrated CRISPR–Cas technique effectively overcomes the core limitations of traditional PCR, and delivers rapid, highly sensitive detection capabilities within a fully integrated, automated "sample-to-answer" solution. This ability to perform the entire diagnostic workflow on a portable chip dramatically reduces hands-on time, minimizes the risk of cross-contamination, and eliminates the need for bulky laboratory equipment. Ultimately, microfluidics-integrated CRISPR–Cas systems transform complex molecular diagnostics into simple, reliable tools, paving the way for widespread, decentralized deployment in POC applications.

4.2. Viruses

The ability to accurately and rapidly detect viruses is critical for global public health, enabling the early diagnosis of infectious diseases, effective outbreak control, and targeted patient treatment.[118,119] The two most common methods for detecting viruses are molecular methods, which are based on the detection of virus genetic material, such as DNA and RNA,[120] and protein tests, which are based on the detection of specific antigens of the virus.[118,121] Molecular methods, such as PCR and reverse transcription PCR (RT-PCR), are considered the gold standard but suffer from expensive thermal cyclers, multiple manual steps, and cross-contamination, as discussed in the above section involving nucleic acid detection. Antigen tests are fast and inexpensive, but they are less sensitive and prone to false negatives, especially early in an infection. This is why microfluidics-integrated CRISPR–Cas systems have emerged as ideal candidates for achieving portable, rapid, reliable, and user-friendly virus detection.

Most frequently, the identification of viruses through microfluidics-integrated CRISPR–Cas systems is realized based on the detection of nucleic acids (DNA or RNA) that are specific to the target virus, which is followed by the signal conversion to obtain the virus concentration. This technique has played an important role in the diagnosis of coronavirus disease 2019 (COVID-19).[122,123] For example, a self-contained microfluidic chip integrates all the necessary steps for molecular diagnostic tests, including isothermal amplification, CRISPR cleavage, and lateral flow detection, into a single chip. Specifically, a low-cost, disposable hand warmer is used to provide the necessary heat for the isothermal amplification reaction, making the system highly portable. The platform achieved the detection of SARS-CoV-2 RNA with an LOD as low as 100 copies per test from clinical samples (Fig. 5A).[103] In another work, a centrifugal microfluidic chip was integrated with RT-LAMP amplification and the CRISPR–Cas12a system to detect viral RNA. The chip was designed in a multi-well plate with individual reaction units, each containing a chamber connected *via* microchannels to two CRISPR–Cas12a detection chambers, allowing simultaneous processing of up to 96 samples. Complemented by a portable imaging device and a deep learning algorithm, the platform realized automated SARS-CoV-2 detection with an LOD as low as 250 copies per mL within 30 min.[104] A notable advancement was a highly integrated, fully enclosed lab-on-a-chip CRISPR system designed to differentiate SARS-CoV-2 variants. This system seamlessly incorporates viral RNA extraction, RPA for amplification, and CRISPR–Cas12a detection into a single device, eliminating manual transfer and minimizing cross-contamination. Its design supported two-sample input with ten parallel detection chambers, enabling the automated identification of SARS-CoV-2 (including BA.1, BA.2, and BA.5 variants), influenza A (H_1N_1, H_3N_2), influenza B (IVB), and human respiratory syncytial virus (HRSV) with an LOD of 100 copies per mL in 60 min (Fig. 5B).[105]

In addition, microfluidics-integrated CRISPR–Cas systems have demonstrated broad applicability in diagnosing other viral infections. For example, a microfluidic dual-droplet device was designed to generate picoliter-sized droplets by combining pressure and vacuum, for the simultaneous detection of HPV nucleic acid targets. The sample was mixed with the reagents for both RPA and CRISPR detection, loaded into the chip and partitioned into two distinct groups of droplets, with each group of droplets containing a specific crRNA for its target. The detection assay generates fluorescence signals, allowing for ultra-sensitive detection of HPV 16 and HPV 18 with LODs down to 0.18 nM and 0.25 nM, respectively, during a total process time of approximately 30 min (Fig. 5C).[106] Later, the same group developed a stand-alone SlipChip integrated with RPA and Cas12a assays to simultaneously detect HPV16 and HPV18, achieving a detection sensitivity of approximately 6 copies per reaction and a reaction time of 36 min.[107] Another work reported a pneumatic microfluidic chip that contained 24 parallel reaction structures and was integrated with a custom-designed fluorometer, for automatic CRISPR–Cas13a-based detection of Ebola virus. This system achieved ultrasensitive detection of the *Ebola* virus with an LOD as low as 20 pfu mL^{-1}, while requiring only 50 μL of blood, 5 min, and $6 per assay (Fig. 5D).[108]

In addition to its critical application in human disease diagnostics, the microfluidics-integrated CRISPR–Cas platform also has significant potential for managing infections affecting plants and livestock. An innovative, portable diagnostic platform that integrates artificial intelligence (AI), CRISPR–Cas14a technology, and centrifugal microfluidics was developed to enable rapid, on-site detection of multiple devastating geminiviruses in tomato plants and whitefly vectors. The viral ssDNA was amplified *via* an asymmetric isothermal reaction and loaded into the centrifugal chip containing separate reaction chambers, thus

© 2025 The Author(s). Published by the Royal Society of Chemistry

Open Access Article. Published on 28 2025. Downloaded on 02.12.2025 02:59:53.
This article is licensed under a Creative Commons Attribution 3.0 Unported Licence.

allowing for the simultaneous detection of four geminiviruses *via* the collateral activity of Cas14a. The generated fluorescence signals were interpreted *via* a machine learning algorithm, enabling target quantification with an ultralow LOD of 10 fM and a significantly reduced reaction time of 5 min (Fig. 5E).[109]

In brief, microfluidics-integrated CRISPR–Cas systems have successfully addressed critical limitations of traditional viral diagnostic methods by creating portable, rapid, highly sensitive, and automated platforms. As evidenced by their successful applications in detecting human viruses, such as SARS-CoV-2, HPV, and Ebola, as well as their expanding potential in agricultural biosecurity, these systems have shown great potential for delivering gold-standard molecular accuracy outside of laboratories, paving the way for their widespread adoption in practical clinical applications.

4.3. Bacteria

Detecting pathogenic bacteria quickly and accurately is paramount for public health, as it is essential for preventing the spread of infectious diseases, ensuring food safety, and, most critically, guiding the appropriate use of antibiotics to combat antimicrobial resistance. Traditional bacterial detection methods mainly include culture-based assays and molecular diagnostic methods.[124,125] Culture-based assays are highly sensitive and can provide drug resistance profiles, but they are notoriously slow, often requiring 24 to 72 hours for results.[126,127] Molecular methods, such as PCR, offer faster results but still suffer from complex manipulation and a high risk of cross-contamination. The emergence of microfluidics-integrated CRISPR–Cas systems has revolutionized the molecular detection modalities. The assay works by quantifying the nucleic acids (DNA and RNA) to reveal the presence and concentration of bacteria, and directly addresses these limitations by eliminating the need for large laboratory equipment, reducing the contamination risk, and enabling rapid, sensitive, and user-friendly diagnostic tools for bacterial identification.[128–130]

The employment of a microfluidic chip offered the possibility of automating sequential operations into a single chip, eliminating cross-contamination. A digital microfluidic chip integrated with an electrode array was designed to manipulate the microdroplets to perform all the assay processes, including cell lysis, nucleic acid amplification, and Cas12a *trans*-cleavage for fluorescence signal output, without

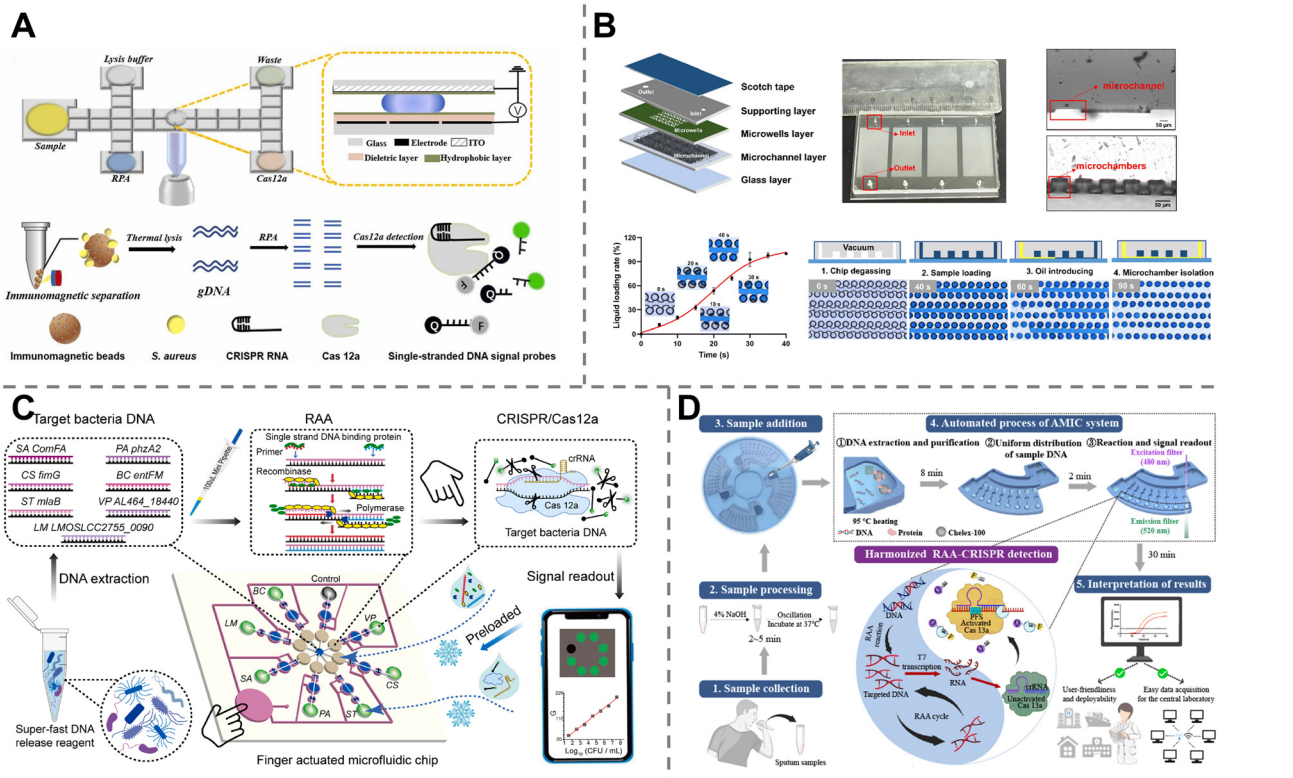

Fig. 6 Microfluidic CRISPR–Cas system for virus detection. (A) A digital microfluidic chip integrated with an electrode array to manipulate the microdroplets for *S. aureus* detection. Reprinted with permission from ref. 110. Copyright 2023 Elsevier. (B) A microwell array-based digital microfluidic platform for the detection of viable *E. coli* O157:H7 in food samples. Reprinted with permission from ref. 111. Copyright 2024 WILEY-VCH Verlag GmbH. (C) A microfluidic chip with eight parallel detection structures radially arranged around the central sample inlet for multiplex detection of 7 foodborne pathogens. Reprinted with permission from ref. 112. Copyright 2023 Elsevier. (D) An "all-in-one" centrifugal microfluidic chip for the simultaneous detection of 12 respiratory bacteria. Reprinted with permission from ref. 113. Copyright 2024 American Chemical Society.

Open Access Article. Published on 28 2025. Downloaded on 02.12.2025 02:59:53. This article is licensed under a Creative Commons Attribution 3.0 Unported Licence.

manual operation. The chip accomplished sensitive detection of *Staphylococcus aureus* (*S. aureus*) from spiked urine and milk samples at an LOD of 32 CFU mL^{-1} within 55 min (Fig. 6A).[110] Moreover, accurate differentiation between viable and non-viable cells should be ensured to avoid false positives caused by the presence of dead bacteria. A microwell array-based digital lab-on-a-chip platform was reported to be highly sensitive and specific for the detection of viable *Escherichia coli* (*E. coli*) O157:H7 in food samples. The chip creatively integrated propidium monoazide (PMA) to enter dead bacteria and modify their DNA, eliminating interference from 99% of the dead bacteria. Thus, the microwells containing live bacteria initiated CRISPR–Cas12a and generated a detectable fluorescence signal, achieving an LOD of 36 CFU mL^{-1} within a drastically reduced detection time of 15 min, due to the enhanced confinement effect within the tiny microwells (Fig. 6B).[111]

Furthermore, the rapid and simultaneous identification of multiple potential pathogens from a single sample is crucial for effective clinical intervention, accelerated outbreak management, and stringent food safety control. Microfluidics-integrated CRISPR platforms, in particular, have significantly advanced the field of bacterial multiplex detection. A novel microfluidic device with eight parallel detection structures radially arranged around and connected to the central sample inlet has been reported to perform multiplex detection of foodborne pathogens. Each structure contained a nucleic acid amplification well, a pneumatic control region, and a CRISPR–Cas detection well, and the fluid movement was controlled by simple finger pressing. The platform achieved the simultaneous detection of *Bacillus cereus*, *Listeria monocytogenes*, *S. aureus*, *Pseudomonas aeruginosa* (*P. aeruginosa*), *S. typhimurium*, *Cronobacter sakazakii*, and *Vibrio parahaemolyticus*, with LODs below 500 CFU mL^{-1} and a detection time of 60 min (Fig. 6C).[112] The integration of the RAA-CRISPR–Cas13a system with a centrifugal microfluidic chip provided an "all-in-one" platform that successfully performed DNA extraction, purification, distribution, amplification, detection and signal output within a single chip. In addition, designed to consist of 32 individual functional units, the chip achieved simultaneous detection of 12 respiratory bacteria with an LOD as low as 10 CFU mL^{-1} (Fig. 6D).[113]

Overall, the integration of microfluidics with CRISPR–Cas systems represents a significant improvement in bacterial diagnostics. These platforms deliver on the promise of fully automated, sample-to-answer analysis, achieving both ultra-high sensitivity and specificity within minutes. By enabling the simultaneous detection of up to 12 pathogens and accurate differentiation between viable and non-viable cells, this technology holds immense promise for effective clinical intervention and the global fight against antimicrobial resistance.

4.4. Other biomarkers

The versatile utility of microfluidics-integrated CRISPR–Cas systems is not confined to the detection of nucleic acids, viral genes and bacterial genes. A variety of recent studies have also demonstrated the innovative expansion of such techniques into detecting other non-genetic biomarkers (such as fungi, mycotoxins, and *Treponema pallidum*), generally by coupling the highly specific nucleic acid recognition capabilities of CRISPR–Cas with sophisticated non-nucleic acid transducers.

Fungi are a diverse group of eukaryotic organisms that include yeasts, molds, and mushrooms. The detection of fungi can be realized by the recognition of target nucleic acids and concentration conversion.[131,132] A carefully designed strategy based on a ruler-readout paper-based microfluidic chip coupled with glucoamylase-embedded DNA hydrogels was proposed for visual quantification of invasive fungi. Initially, both CRISPR–Cas detection reagents and the sample were encapsulated into a DNA hydrogel. In the presence of the target 18S rRNA of the target fungi, the *trans*-cleavage activity of the Cas12a proteins was activated, cleaving the DNA linkers, destroying the hydrogel scaffold, and releasing the pre-embedded glucoamylase. The released glucoamylase then catalyzed the hydrolysis of amylose and produced glucose in the hydrogel supernatant, which was introduced into the ruler-readout μPAD and induced a readable colorimetric signal. Based on this platform, ultra-sensitive detection of *Candida* and *Aspergillus* has been achieved, with LODs of 4.90 and 4.13 CFU mL^{-1}, respectively (Fig. 7A).[114]

Mycotoxins are toxic secondary metabolites produced by certain species of fungi that pose a serious threat to human and animal health. Mycotoxin detection is crucial in the food safety monitoring and agricultural industries.[133–135] Although mycotoxins do not possess genes or proteins, they can be detected on the basis of signal transduction, for example, by converting the target concentration to the quantity of CRISPR activator using aptamers and complementary strands.[136,137] An electrochemical centrifugal microfluidic chip was developed for the detection of ochratoxin A (OTA), a harmful mycotoxin found in food. The chip was integrated with a reaction area, a detection area and a screen-printed gold electrode functionalized with Pd@PCN-222-labelled ssDNA probes. Pd@PCN-222 exhibited peroxidase-like activity and could catalyze the reduction of H_2O_2. During detection, the presence of OTA resulted in the competitive binding and the release of a complementary strand that would bind to the crRNA and activate the non-specific *trans*-cleavage activity of the Cas12a proteins. The activated Cas12a randomly cleaved the Pd@PCN-222-labelled ssDNA on the electrode surface and thus reduced the peroxidase activity toward the reduction peak current of H_2O_2. The generated electrochemical signals were measured to determine the OTA concentration. The platform without pre-amplification has achieved an excellent LOD of 1.21 pg mL^{-1} (Fig. 7B).[115]

The integration of advanced functional nanomaterials with microfluidic CRISPR–Cas systems has enabled novel

© 2025 The Author(s). Published by the Royal Society of Chemistry

Open Access Article. Published on 28 2025. Downloaded on 02.12.2025 02:59:53.
This article is licensed under a Creative Commons Attribution 3.0 Unported Licence.

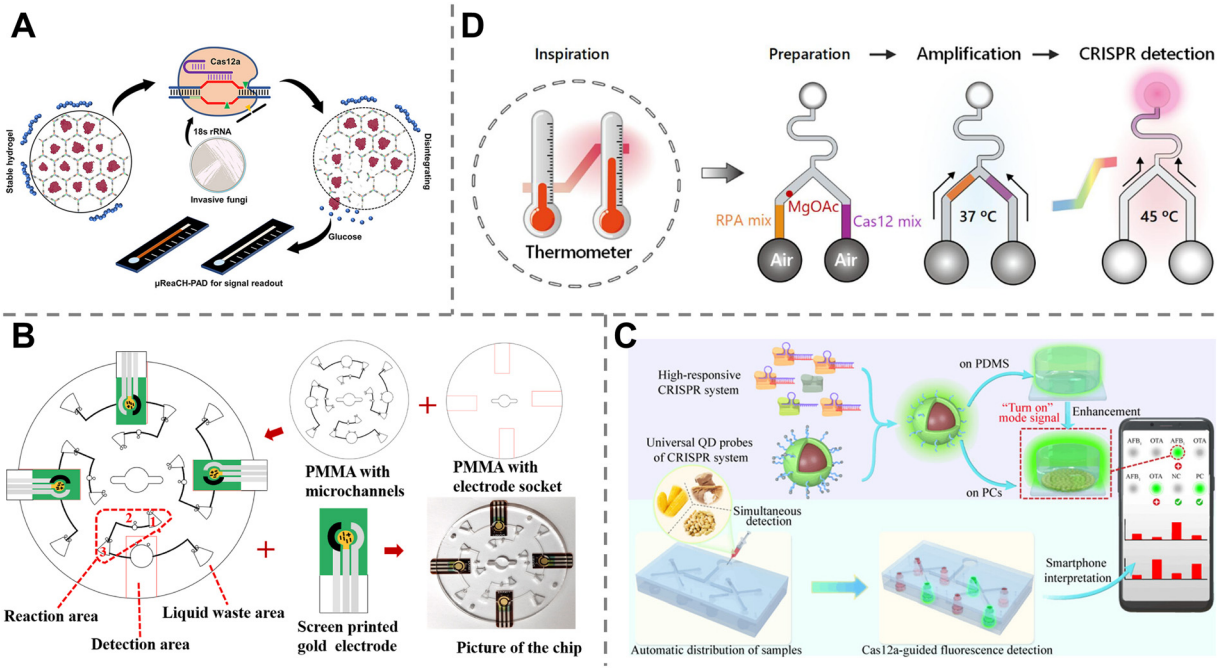

Fig. 7 Microfluidic CRISPR–Cas system for the detection of other biomarkers. (A) A ruler-readout paper-based microfluidic chip coupled with glucoamylase-embedded DNA hydrogels for visual quantification of invasive fungi. Reprinted with permission from ref. 114. Copyright 2021 American Chemical Society. (B) An electrochemical centrifugal microfluidic chip integrated with Pd@PCN-222 nanoparticles for ochratoxin A detection. Reprinted with permission from ref. 115. Copyright 2024 Elsevier. (C) A microfluidic chip modified with photonic crystals and CdSe/ZnS QDs for simultaneous detection of 6 mycotoxins. Reprinted with permission from ref. 116. Copyright 2023 American Chemical Society. (D) A microfluidic chip based on temperature-programmed air expansion for automated detection of *Treponema pallidum*. Reprinted with permission from ref. 117. Copyright 2024 Elsevier.

approaches for signal conversion and amplification. For instance, CdSe/ZnS quantum dots (QDs), functionalized with a quenched reporter strand, were used as signal transducers on a microfluidic chip. Upon target mycotoxin recognition, the released activator triggered the *trans*-cleavage activity of Cas12a, which also cleaved the reporters on the QD surface and restored their green fluorescence. The reaction chambers in the microfluidic chip, modified with photonic crystals, further enhanced the fluorescence signal. Combined with smartphone-based detection, this strategy enabled simultaneous quantification of six mycotoxins, including aflatoxin B_1 (AFB_1), OTA, zearalenone (ZEN), fumonisin B_1 (FB_1), T-2 mycotoxin (T-2), and deoxynivalenol (DON), achieving LODs as low as 2.3, 3.9, 2.6, 1.4, 1.7, and 1.5 fg mL^{-1}, respectively, within 40 min (Fig. 7C).[116]

Moreover, microfluidics-integrated CRISPR–Cas systems can also be employed for the detection of other pathogens. An automated RPA-CRISPR–Cas12a assay platform for *Treponema pallidum* (the spirochete causing syphilis) has been developed. This platform utilized a cleverly designed microfluidic chip that precisely manipulates fluid flow and reagent mixing through temperature-programmed air expansion. Initially, the RPA and CRISPR reagents were preloaded into two separate chambers on the chip. Upon heating, the expanded air acts as a piston, pushing the two sets of reagents together to mix, thereby activating the CRISPR detection of the target DNA. Integrated with a smartphone for automated data analysis, this all-in-one platform achieved the detection of *Treponema pallidum* with an LOD of 10 copies per μL in approximately 30 min (Fig. 7D).[117]

While CRISPR–Cas systems have been extensively applied for protein detection through nucleic acid signal transduction mechanisms,[138,139] the integration of such CRISPR-based protein sensing strategies with microfluidic platforms remains an emerging area. A notable related work by Song *et al.* reported the CRISPR–Cas12a-based detection of telomerase activity in a single-cell microfluidic chip, with the utilization of DNA-functionalized UiO-66 nanoparticles as signal transducers.[140] This pioneering demonstration highlights the feasibility of coupling enzymatic activity assays[141] with microfluidics-integrated CRISPR–Cas systems and suggests the future efforts toward direct, multiplexed, and automated protein detection.

In brief, by strategically coupling the robust *trans*-cleavage activity of Cas proteins and innovative non-nucleic acid transducers, such as DNA hydrogels, aptamers, and functional nanomaterials, researchers have successfully developed microfluidics-integrated CRISPR–Cas platforms capable of detecting a far broader range of critical biomarkers. These advances demonstrate that the technique holds promise as a versatile sensing tool applicable across diverse fields, from clinical diagnostics to food safety and environmental monitoring.

© 2025 The Author(s). Published by the Royal Society of Chemistry

Open Access Article. Published on 28 2025. Downloaded on 02.12.2025 02:59:53.
This article is licensed under a Creative Commons Attribution 3.0 Unported Licence.

5. Conclusions and perspectives

In this review, we highlight the revolutionary advances in molecular diagnostics achieved by the combination of microfluidics and CRISPR–Cas systems, leveraging the unparalleled specificity, programmability, and collateral cleavage-based signal amplification of CRISPR–Cas systems, in combination with the miniaturization, automation, and multiplexing of microfluidic devices. A variety of novel and powerful diagnostic platforms have been developed based on different microfluidic devices, including centrifugal microfluidic chips, microdroplets, microfluidic array chips, paper-based microfluidic chips, and electrochemical chips, and successfully enabled ultrasensitive detection of nucleic acids, viruses, bacteria, mycotoxins, *etc.* Notable breakthroughs lie in the ability to incorporate multiple steps in a single chip, which not only minimizes the risk of cross-contamination but also automates the entire workflow. In addition, the ability to detect multiple biomarkers simultaneously in one assay also enhances the detection efficiency. Collectively, these advances pave the way for realizing fully integrated, true "sample-to-answer" POC diagnostics.

Despite remarkable progress, several challenges remain, which hamper the practical implementation of microfluidics-integrated CRISPR–Cas platforms for clinical diagnostics. First, sample preparation is one of the major bottlenecks, as fully integrating and automating all crucial steps, especially nucleic acid extraction and cell lysis from biological matrices (*e.g.*, blood, saliva, and swabs) is difficult. Second, on-chip multiplexing requires the careful design of not only chip structures, but also multiple guide RNAs and signal reporters, which introduces risk of cross-reactivity and arduous signal interpretation. Therefore, although microfluidic systems promise cost-effective testing, the fabrication and large-scale manufacturing of multifunctional modules, such as valves, pumps and signal interpreters, remain technically demanding and expensive, which further limits the applicability of these devices in low-resource or POC settings. Third, the great majority of current studies are conducted under controlled laboratory conditions rather than diverse patient populations, thus the clinical validation is still limited. The lack of standardized protocols and inter-platform validation ensuring reliable result comparison also impedes the reproducibility and regulatory approval of these devices before consistent clinical deployment. Finally, scaling up production to achieve mass manufacturability while maintaining performance uniformity and cost-effectiveness remains the last significant challenge for translating microfluidics-integrated CRISPR–Cas platforms from laboratory to real-world diagnostics.

In the future, efforts should focus on the key aspects addressing these challenges, such as the improvement of portability, the convergence of artificial intelligence, the exploration of new Cas proteins, and the standardization for commercialization.

The development of fully integrated and passive systems that eliminate the need for sequential manual operations, external power sources, and bulky signal readout instruments, will enable true "sample-to-answer" workflows. Such platforms should seamlessly incorporate all necessary steps within a single device, including sample loading, target extraction, amplification, reagent mixing, detection, signal transduction, result interpretation, and output. In addition to achieving complete automation, future diagnostic tools must also prioritize miniaturization, portability, and low cost to ensure practical applicability. In this regard, passive microfluidic chips driven by capillary action or gravitational force represent particularly promising candidates. This transition is essential not only for reducing costs and enhancing user-friendliness but also for expanding accessibility to resource-limited and field-deployable settings.

In parallel, the convergence of artificial intelligence with microfluidics-based CRISPR–Cas devices will open new horizons. By embedding portable optical readers, electrochemical sensors, or smartphone cameras into microfluidic devices, raw signals can be rapidly collected and transmitted for data processing. Coupled with AI and machine learning algorithms, these platforms will provide automated pattern recognition, noise filtering, and quantitative analysis, thereby not only significantly reducing the data processing time, but also reducing false positives and negatives. Besides, AI-driven models can also incorporate patient history and contextual data to enable real-time data transmission, remote interpretation, and large-scale epidemiological monitoring, which facilitates predictive diagnostic insights and personalized recommendations. Such intelligent and data-driven diagnostic tools, achieved by integrating smartphones, wireless communication, AI, cloud-based platforms, will greatly enhance the accuracy, automation, and accessibility of CRISPR-based POCT.

Another important research direction is the exploration of Cas proteins beyond the widely used Cas12 and Cas13 proteins. Emerging candidates such as Cas14 and Casϕ represent promising alternatives for future diagnostic platforms. Owing to their smaller size, these proteins are easier to incorporate into compact devices, whereas their broader target recognition range and stronger collateral cleavage activity provide enhanced signal amplification. When coupled with high-throughput microfluidic systems, such as droplet-based platforms or microarray chips, and advanced encoding strategies, these CRISPR–Cas systems can enable simultaneous screening of dozens or even hundreds of pathogens or disease-related genes in a single test, thereby significantly improving detection efficiency and expanding the overall diagnostic value of CRISPR-based technologies.

Finally, standardization and commercialization remain crucial for translating microfluidics-integrated CRISPR–Cas diagnostic platforms from laboratory prototypes into practical applications. Future research efforts should not only focus on technical innovation but also address challenges in the establishment of standardized validation protocols, large-

© 2025 The Author(s). Published by the Royal Society of Chemistry

Open Access Article. Published on 28 2025. Downloaded on 02.12.2025 02:59:53.
This article is licensed under a Creative Commons Attribution 3.0 Unported Licence.

scale and cost-effective manufacturing, strict quality control, and long-term stability of reagents and microfluidic chips under diverse storage and transport conditions. In addition, the development of user-friendly interfaces and simplified workflows will be essential to meet the needs of clinicians and non-specialist users. To this end, close collaboration among academic researchers, clinicians, regulatory agencies, and industrial partners will be vital to ensure clinical reliability, regulatory approval, and promotion of market-ready products capable of deployment in both healthcare and community settings.

Overall, by advancing in these directions, microfluidics-integrated CRISPR–Cas diagnostics are poised to evolve into highly reliable, user-friendly, and globally accessible tools, with the potential to transform disease detection, public health surveillance, and precision medicine in the coming years.

Author contributions

Yanping Wang: funding acquisition, investigation, methodology, and writing – original draft. Huimin Jiang: validation and writing – original draft. Yanyin Zhang: validation and writing – original draft. Qingran Yang: writing – review and editing. Yujun Song: conceptualization, funding acquisition, supervision, and writing – review and editing. Yanfeng Gao: conceptualization, funding acquisition, investigation, methodology, supervision, and writing – review and editing.

Conflicts of interest

There are no conflicts to declare.

Abbreviation list

AI	Artificial intelligence
AFB_1	Aflatoxin B_1
ATP	Adenosine triphosphate
COF	Covalent organic framework
COVID-19	Coronavirus disease 2019
crRNA	CRISPR RNA
CRISPR	Clustered regularly interspaced short palindromic repeats
Cas	CRISPR-associated proteins
dLAMP	Digital loop-mediated isothermal amplification
DNA	Deoxyribonucleic acid
DON	Deoxynivalenol
E. coli	*Escherichia coli*
FB_1	Fumonisin B_1
GOx	Glucose oxidase
gRNA	Guide RNA
HPV	Human papillomavirus
HRSV	Human respiratory syncytial virus
LAMP	Loop-mediated isothermal amplification
LFD	Lateral flow dipstick
LOD	Limit of detection
MOF	Metal–organic framework
NGS	Next-generation sequencing
OTA	Ochratoxin A
PAM	Protospacer adjacent motif
PCR	Polymerase chain reaction
PFS	Protospacer flanking site
PMA	Propidium monoazide
PMMA	Poly(methyl methacrylate)
POC	Point-of-care
POCT	Point-of-care testing
QD	Quantum dot
RAA	Recombinase-aided amplification
RPA	Recombinase polymerase amplification
RT-PCR	Reverse transcription polymerase chain reaction
S. aureus	*Staphylococcus aureus*
ssDNA	Single-stranded DNA
ssRNA	Single-stranded RNA
SARS-CoV-2	Severe acute respiratory syndrome coronavirus 2
S. typhimurium	*Salmonella typhimurium*
ZEN	Zearalenone
μPAD	Microfluidic paper-based analytical device

Data availability

No primary research results, software or code have been included and no new data were generated or analysed as part of this review.

Acknowledgements

This work was funded by the National Natural Science Foundation of China (22477056 and 82572370), the National Key Research and Development Program of China (2019YFA0709200), the Jiangsu Provincial Key Research and Development Program (BE2021373), the Natural Science Foundation of Anhui Province (2408085QH276), the Scientific Research Foundation of Education Department of Anhui Province of China (2024AH051909 and 2024AH051911), the Fundamental Research Funds for the Central Universities (3332023076) and the State Key Laboratory of Analytical Chemistry for Life Science (5431ZZXM2304).

References

1 Y. Zhu, K. Li, J. Zhang, L. Wang, L. Sheng and L. Yan, *Transl. Cancer Res.*, 2021, **10**, 1193–1203.
2 M. Pan, P. Chen, Q. Zhang, Y. Yang, W. Hu, G. Hu, R. Wang and X. Chen, *Transl. Cancer Res.*, 2024, **13**, 330–347.
3 Y. Gao, Y. Wang, J. Zhao and Y. Song, *Acta Pharm. Sin. B*, 2024, **14**, 3780–3782.
4 D. Zhou, Z. Zhang, L. Pan, Y. Wang, J. Yang, Y. Gao and Y. Song, *Angew. Chem., Int. Ed.*, 2024, **63**, e202404493.
5 A. Afzal, *J. Adv. Res.*, 2020, **26**, 149–159.
6 A. Tahamtan and A. Ardebili, *Expert Rev. Mol. Diagn.*, 2020, **20**, 453–454.

Open Access Article. Published on 28 2025. Downloaded on 02.12.2025 02:59:53.
This article is licensed under a Creative Commons Attribution 3.0 Unported Licence.

7 H. Satam, K. Joshi, U. Mangrolia, S. Waghoo, G. Zaidi, S. Rawool, R. P. Thakare, S. Banday, A. K. Mishra, G. Das and S. K. Malonia, *Biology*, 2023, **12**, 997.
8 J. A. Doudna and E. Charpentier, *Science*, 2014, **346**, 1258096.
9 M. Jinek, K. Chylinski, I. Fonfara, M. Hauer, J. A. Doudna and E. Charpentier, *Science*, 2012, **337**, 816–821.
10 J. E. van Dongen, J. T. W. Berendsen, R. D. M. Steenbergen, R. M. F. Wolthuis, J. C. T. Eijkel and L. I. Segerink, *Biosens. Bioelectron.*, 2020, **166**, 112445.
11 J. S. Gootenberg, O. O. Abudayyeh, J. W. Lee, P. Essletzbichler, A. J. Dy, J. Joung, V. Verdine, N. Donghia, N. M. Daringer, C. A. Freije, C. Myhrvold, R. P. Bhattacharyya, J. Livny, A. Regev, E. V. Koonin, D. T. Hung, P. C. Sabeti, J. J. Collins and F. Zhang, *Science*, 2017, **356**, 438–442.
12 J. P. Broughton, X. Deng, G. Yu, C. L. Fasching, V. Servellita, J. Singh, X. Miao, J. A. Streithorst, A. Granados, A. Sotomayor-Gonzalez, K. Zorn, A. Gopez, E. Hsu, W. Gu, S. Miller, C.-Y. Pan, H. Guevara, D. A. Wadford, J. S. Chen and C. Y. Chiu, *Nat. Biotechnol.*, 2020, **38**, 870–874.
13 H. Li, J. Yang, G. Wu, Z. Weng, Y. Song, Y. Zhang, J. A. Vanegas, L. Avery, Z. Gao, H. Sun, Y. Chen, K. D. Dieckhaus, X. Gao and Y. Zhang, *Angew. Chem., Int. Ed.*, 2022, **61**, e202203826.
14 C. Myhrvold, C. A. Freije, J. S. Gootenberg, O. O. Abudayyeh, H. C. Metsky, A. F. Durbin, M. J. Kellner, A. L. Tan, L. M. Paul, L. A. Parham, K. F. Garcia, K. G. Barnes, B. Chak, A. Mondini, M. L. Nogueira, S. Isern, S. F. Michael, I. Lorenzana, N. L. Yozwiak, B. L. MacInnis, I. Bosch, L. Gehrke, F. Zhang and P. C. Sabeti, *Science*, 2018, **360**, 444–448.
15 H. Li, Y. Xie, F. Chen, H. Bai, L. Xiu, X. Zhou, X. Guo, Q. Hu and K. Yin, *Chem. Soc. Rev.*, 2023, **52**, 361–382.
16 S. Del Giovane, N. Bagheri, A. C. Di Pede, A. Chamorro, S. Ranallo, D. Migliorelli, L. Burr, S. Paoletti, H. Altug and A. Porchetta, *TrAC, Trends Anal. Chem.*, 2024, **172**, 117594.
17 A. Ghouneimy, A. Mahas, T. Marsic, R. Aman and M. Mahfouz, *ACS Synth. Biol.*, 2023, **12**, 1–16.
18 Y. Gao, P. Magaud, L. Baldas, C. Lafforgue, M. Abbas and S. Colin, *Microfluid. Nanofluid.*, 2017, **21**, 154.
19 Y. Gao, P. Magaud, C. Lafforgue, S. Colin and L. Baldas, *Microfluid. Nanofluid.*, 2019, **23**, 93.
20 M. Abbas, P. Magaud, Y. Gao and S. Geoffroy, *Phys. Fluids*, 2014, **26**, 123301.
21 F. Cui, M. Rhee, A. Singh and A. Tripathi, *Annu. Rev. Biomed. Eng.*, 2015, **17**, 267–286.
22 Y. Yang, Y. Chen, H. Tang, N. Zong and X. Jiang, *Small Methods*, 2020, **4**, 1900451.
23 W. Jung, J. Han, J.-W. Choi and C. H. Ahn, *Microelectron. Eng.*, 2015, **132**, 46–57.
24 Y. Gao, D. Zhou, Q. Xu, J. Li, W. Luo, J. Yang, Y. Pan, T. Huang, Y. Wang, B. He, Y. Song and Y. Wang, *ACS Appl. Mater. Interfaces*, 2023, **15**, 5010–5018.
25 Y. Wang, Y. Gao and Y. Song, *ChemMedChem*, 2022, **17**, e202200422.
26 W. Bi, X. Cao, J. Li, Y. Gao, Y. Song and B. He, *ACS Sens.*, 2025, **10**, 2136–2146.
27 X. Luan, Y. Gao, Y. Pan, Z. Huang, F. Zeng, G. He, B. He, D. Ye and Y. Song, *Anal. Chem.*, 2025, **97**, 3395–3403.
28 Y. Gao, Y. Wang, X. Liu, Z. Zhu, Z. Li, Z. Zhang, Y. Yin, W. C. S. Cho, Y. Song and Y. Wang, *Anal. Chim. Acta*, 2023, **1241**, 340806.
29 A. Wang, X. Liu, S. Feng, Y. Wang, Y. Song and Y. Gao, *ChemBioChem*, 2025, **26**, e202400807.
30 Y. Gao, Y. Wang, Y. Wang, P. Magaud, Y. Liu, F. Zeng, J. Yang, L. Baldas and Y. Song, *TrAC, Trends Anal. Chem.*, 2023, **158**, 116887.
31 Y. Gao, Y. Wang, B. He, Y. Pan, D. Zhou, M. Xiong and Y. Song, *Angew. Chem., Int. Ed.*, 2023, **62**, e202302000.
32 H. Yue, M. Huang, T. Tian, E. Xiong and X. Zhou, *ACS Nano*, 2021, **15**, 7848–7859.
33 M. Azimzadeh, M. Mousazadeh, A. Jahangiri-Manesh, P. Khashayar and P. Khashayar, *Chem*, 2021, **10**, 3.
34 F. Nafian, K. S. Esfahani, M. Hobabi Aghmiuni, S. Khoushab, T. Illeslamllo, S. Nafian, N. Mohamadiyan, N. S. Aleyasin and B. Kamali Doust Azad, *Anal. Methods*, 2025, **17**, 497–507.
35 S. Feng, Y. Zhang, Y. Gao, Y. Liu, Y. Wang, X. Han, T. Zhang and Y. Song, *Angew. Chem., Int. Ed.*, 2023, **62**, e202313968.
36 S. Feng, Y. Zhang, Y. Wang, Y. Gao and Y. Song, *Chem. – Eur. J.*, 2024, **30**, e202402485.
37 E. V. Koonin and K. S. Makarova, *Philos. Trans. R. Soc., B*, 2019, **374**, 20180087.
38 F. Jiang and J. A. Doudna, *Annu. Rev. Biophys.*, 2017, **46**, 505–529.
39 P. M. Nussenzweig and L. A. Marraffini, *Annu. Rev. Genet.*, 2020, **54**, 93–120.
40 R. Barrangou, *Curr. Opin. Immunol.*, 2015, **32**, 36–41.
41 L. Li, G. Shen, M. Wu, J. Jiang, Q. Xia and P. Lin, *Trends Biotechnol.*, 2022, **40**, 1326–1345.
42 M. M. Kaminski, O. O. Abudayyeh, J. S. Gootenberg, F. Zhang and J. J. Collins, *Nat. Biomed. Eng.*, 2021, **5**, 643–656.
43 Q. Zhao, B. Pan, W. Long, Y. Pan, D. Zhou, X. Luan, B. He, Y. Wang and Y. Song, *Nano Lett.*, 2022, **22**, 9714–9722.
44 Y. Yang, X. Li, X. Wang, Z. Wang and S. Gong, *TrAC, Trends Anal. Chem.*, 2025, **182**, 118058.
45 J. Ki, H.-K. Na, S. W. Yoon, V. P. Le, T. G. Lee and E.-K. Lim, *ACS Sens.*, 2022, **7**, 3940–3946.
46 P. D. Priya Swetha, J. Sonia, K. Sapna and K. S. Prasad, *Curr. Opin. Electrochem.*, 2021, **30**, 100829.
47 J. Ma, X. Li, C. Lou, X. Lin, Z. Zhang, D. Chen and S. Yang, *Anal. Methods*, 2023, **15**, 3785–3801.
48 Y. Pan, X. Luan, F. Zeng, Q. Xu, Z. Li, Y. Gao, X. Liu, X. Li, X. Han, J. Shen and Y. Song, *Biosens. Bioelectron.*, 2022, **209**, 114239.
49 W. Long, J. Yang, Q. Zhao, Y. Pan, X. Luan, B. He, X. Han, Y. Wang and Y. Song, *Anal. Chem.*, 2023, **95**, 1618–1626.
50 Z. Li, Y. Bai, M. You, J. Hu, C. Yao, L. Cao and F. Xu, *Biosens. Bioelectron.*, 2021, **177**, 112952.

© 2025 The Author(s). Published by the Royal Society of Chemistry

Open Access Article. Published on 28 2025. Downloaded on 02.12.2025 02:59:53.
This article is licensed under a Creative Commons Attribution 3.0 Unported Licence.

51 O. Strohmeier, M. Keller, F. Schwemmer, S. Zehnle, D. Mark, F. Von Stetten, R. Zengerle and N. Paust, *Chem. Soc. Rev.*, 2015, **44**, 6187–6229.
52 J. F. Hess, S. Zehnle, P. Juelg, T. Hutzenlaub, R. Zengerle and N. Paust, *Lab Chip*, 2019, **19**, 3745–3770.
53 Y. Xiao, M. Zhou, C. Liu, S. Gao, C. Wan, S. Li, C. Dai, W. Du, X. Feng, Y. Li, P. Chen and B.-F. Liu, *Biosens. Bioelectron.*, 2024, **255**, 116240.
54 R. Burger, D. Kurzbuch, R. Gorkin, G. Kijanka, M. Glynn, C. McDonagh and J. Ducrée, *Lab Chip*, 2015, **15**, 378–381.
55 S. Wang, H. Duan and J. Lin, *Sens. Actuators, B*, 2023, **393**, 134223.
56 T. Shu, X. Yin, Q. Xiong, C. Hua, J. Bu, K. Yang, J. Zhao, Y. Liu, L. Zhu and C. Zhu, *Biosens. Bioelectron.*, 2025, **274**, 117178.
57 Y. Chen, N. Zong, F. Ye, Y. Mei, J. Qu and X. Jiang, *Anal. Chem.*, 2022, **94**, 9603–9609.
58 R. Peng, Z. Lu, M. Liu and F. Hu, *Sens. Actuators, B*, 2024, **399**, 134838.
59 Y. Shang, G. Xing, J. Lin, Y. Li, Y. Lin, S. Chen and J.-M. Lin, *Biosens. Bioelectron.*, 2024, **243**, 115771.
60 X. Ding, K. Yin, Z. Li, M. M. Sfeir and C. Liu, *Biosens. Bioelectron.*, 2021, **184**, 113218.
61 S. Liu, T. Yu, L. Song, K. Kalantar-Zadeh and G. Liu, *ACS Sens.*, 2025, **10**, 4569–4579.
62 R. Bruch, J. Baaske, C. Chatelle, M. Meirich, S. Madlener, W. Weber, C. Dincer and G. A. Urban, *Adv. Mater.*, 2019, **31**, 1905311.
63 E. M. Payne, D. A. Holland-Moritz, S. Sun and R. T. Kennedy, *Lab Chip*, 2020, **20**, 2247–2262.
64 Y. Ding, P. D. Howes and A. J. deMello, *Anal. Chem.*, 2020, **92**, 132–149.
65 Z. Wei, Y. Li, R. G. Cooks and X. Yan, *Annu. Rev. Phys. Chem.*, 2020, **71**, 31–51.
66 L. Bai, Y. Fu, M. Yao and Y. Cheng, *Chem. Eng. J.*, 2018, **332**, 537–547.
67 J. Chi, Y. Wei, J. Chen, L. Ding, X. Chen, X. Wang, J. Xu and C. Peng, *Chem. Eng. J.*, 2025, **523**, 168333.
68 C.-H. Lin, Y.-H. Hsiao, H.-C. Chang, C.-F. Yeh, C.-K. He, E. M. Salm, C. Chen, I.-M. Chiu and C.-H. Hsu, *Lab Chip*, 2015, **15**, 2928–2938.
69 C. Soitu, A. Feuerborn, A. N. Tan, H. Walker, P. A. Walsh, A. A. Castrejón-Pita, P. R. Cook and E. J. Walsh, *Proc. Natl. Acad. Sci. U. S. A.*, 2018, **115**, E5926–E5933.
70 M. Nourmohammadzadeh, Y. Xing, J. W. Lee, M. A. Bochenek, J. E. Mendoza-Elias, J. J. McGarrigle, E. Marchese, Y. Chun-Chieh, D. T. Eddington, J. Oberholzer and Y. Wang, *Lab Chip*, 2016, **16**, 1466–1472.
71 K. Yang, S. Zong, Y. Zhang, Z. Qian, Y. Liu, K. Zhu, L. Li, N. Li, Z. Wang and Y. Cui, *ACS Appl. Mater. Interfaces*, 2020, **12**, 1395–1403.
72 S. W. Han, E. Jang and W.-G. Koh, *Sens. Actuators, B*, 2015, **209**, 242–251.
73 Y. Sun, Y. Huang, T. Qi, Q. Jin, C. Jia, J. Zhao, S. Feng and L. Liang, *ACS Omega*, 2022, **7**, 1819–1826.
74 D. M. Cate, J. A. Adkins, J. Mettakoonpitak and C. S. Henry, *Anal. Chem.*, 2015, **87**, 19–41.
75 Y. He, Y. Wu, J.-Z. Fu and W.-B. Wu, *RSC Adv.*, 2015, **5**, 78109–78127.
76 M. A. Chowdury and F. Khalid, *Int. J. Energy Res.*, 2021, **45**, 18275–18280.
77 K. Yamada, H. Shibata, K. Suzuki and D. Citterio, *Lab Chip*, 2017, **17**, 1206–1249.
78 J. Zhuang, Z. Zhao, K. Lian, L. Yin, J. Wang, S. Man, G. Liu and L. Ma, *Biosens. Bioelectron.*, 2022, **207**, 114167.
79 W. B. Zimmerman, *Chem. Eng. Sci.*, 2011, **66**, 1412–1425.
80 A. Fernández-la-Villa, D. F. Pozo-Ayuso and M. Castaño-Álvarez, *Curr. Opin. Electrochem.*, 2019, **15**, 175–185.
81 A. Gencoglu and A. R. Minerick, *Microfluid. Nanofluid.*, 2014, **17**, 781–807.
82 C. K. Tang, A. Vaze, M. Shen and J. F. Rusling, *ACS Sens.*, 2016, **1**, 1036–1043.
83 D. Feng, L. Li, J. Zhao and Y. Zhang, *Anal. Biochem.*, 2015, **482**, 48–54.
84 T. Li, J. A. Díaz-Real and T. Holm, *Adv. Mater. Technol.*, 2021, **6**, 2100569.
85 J. Chen, D. Yang, D. Ji, B. Guo, Y. Guo, H. Lin, R. Zhang, Z. Chang, Y. Lu, G. Zhu, L. Zhao, T. Rungrotmongkol, X. Lu, Q. Ren, W. Wu, Y. Zhang and Y. Fang, *Adv. Funct. Mater.*, 2025, **35**, 2420701.
86 Q. Luo, Z. Yu, W. Lyu, Y. Luo, L. Xu and F. Shen, *Adv. Sens. Res.*, 2025, **4**, e00030.
87 L. Tian, Y. Gao, Y. Lu, F. Xu, Z. Feng, L. Zi, Z. Deng and J. Yang, *Lab Chip*, 2025, **25**(22), 5762–5776.
88 X. Liu, Y. Wang, Y. Gao and Y. Song, *Analyst*, 2021, **146**, 1115–1126.
89 Y. Han, X. Liu, Q. Zhao, Y. Gao, D. Zhou, W. Long, Y. Wang and Y. Song, *Analyst*, 2022, **147**, 2500–2507.
90 N. Shao, X. Han, Y. Song, P. Zhang and L. Qin, *Anal. Chem.*, 2019, **91**, 12384–12391.
91 H. Wu, S. Qian, C. Peng, X. Wang, T. Wang, X. Zhong, Y. Chen, Q. Yang, J. Xu and J. Wu, *ACS Sens.*, 2021, **6**, 4048–4056.
92 E. M. Hassan and M. C. DeRosa, *TrAC, Trends Anal. Chem.*, 2020, **124**, 115806.
93 H. Schwarzenbach, D. S. B. Hoon and K. Pantel, *Nat. Rev. Cancer*, 2011, **11**, 426–437.
94 A. Niemz, T. M. Ferguson and D. S. Boyle, *Trends Biotechnol.*, 2011, **29**, 240–250.
95 Z. Xu, D. Chen, T. Li, J. Yan, J. Zhu, T. He, R. Hu, Y. Li, Y. Yang and M. Liu, *Nat. Commun.*, 2022, **13**, 6480.
96 X. Shan, F. Gong, Y. Yang, J. Qian, Z. Tan, S. Tian, Z. He and X. Ji, *Anal. Chem.*, 2023, **95**, 16489–16495.
97 R. Bruch, M. Johnston, A. Kling, T. Mattmüller, J. Baaske, S. Partel, S. Madlener, W. Weber, G. A. Urban and C. Dincer, *Biosens. Bioelectron.*, 2021, **177**, 112887.
98 H. Zhou, Z. Xu, L. He, Z. Wang, T. Zhang, T. Hu, F. Huang, D. Chen, Y. Li, Y. Yang and X. Huang, *Anal. Chem.*, 2023, **95**, 3379–3389.
99 Z. Yu, L. Xu, W. Lyu and F. Shen, *Lab Chip*, 2022, **22**, 2954–2961.

Open Access Article. Published on 28 2025. Downloaded on 02.12.2025 02:59:53.
This article is licensed under a Creative Commons Attribution 3.0 Unported Licence.

100 Z. Zhao, R. Wang, X. Yang, J. Jia, Q. Zhang, S. Ye, S. Man and L. Ma, *ACS Nano*, 2024, **18**, 33505–33519.
101 S. Zhao, Y. Zhang, Y. Wang, Z. Ren, P. Wei, T. Zhang, R. Peng, H. Zhou and F. Hu, *Biosens. Bioelectron.*, 2025, **289**, 117886.
102 Y. Zhang, Y. Guo, G. Liu, S. Zhou, R. Su, Q. Ma, Y. Ge, Y.-Q. Lu, L. Cui and G. Wang, *Lab Chip*, 2024, **24**, 3367–3376.
103 Z. Li, X. Ding, K. Yin, L. Avery, E. Ballesteros and C. Liu, *Biosens. Bioelectron.*, 2022, **199**, 113865.
104 L. Zhang, H. Wang, S. Yang, J. Liu, J. Li, Y. Lu, J. Cheng and Y. Xu, *ACS Nano*, 2024, **18**, 24236–24251.
105 J. Shen, Z. Chen, R. Xie, J. Li, C. Liu, Y. He, X. Ma, H. Yang and Z. Xie, *Biosens. Bioelectron.*, 2023, **237**, 115523.
106 Y. Zhao, D. Chen, Z. Xu, T. Li, J. Zhu, R. Hu, G. Xu, Y. Li, Y. Yang and M. Liu, *Anal. Chem.*, 2023, **95**, 3476–3485.
107 Y. Zhao, Z. Li, T. Li, R. Rao, J. Zhu, R. Hu, G. Xu, Y. Li and Y. Yang, *Anal. Chem.*, 2024, **96**, 20602–20611.
108 P. Qin, M. Park, K. J. Alfson, M. Tamhankar, R. Carrion, J. L. Patterson, A. Griffiths, Q. He, A. Yildiz, R. Mathies and K. Du, *ACS Sens.*, 2019, **4**, 1048–1054.
109 Z. Huang, G. Ma, R. Hu, J. Xu, Y. Fu, J. Tang, D. Li, Z. Chen, X. Shentu, Z. Ye, K. Sun and X. Yu, *Chem. Eng. J.*, 2025, **520**, 165904.
110 L. Lu, H. Zhang, F. Lin, L. Zhou, Z. Zhu and C. Yang, *Sens. Actuators, B*, 2023, **381**, 133409.
111 W. Yin, K. Hu, B. Yu, T. Zhang, H. Mei, B. Zhang, Z. Zou, L. Xia, Y. Gui, J. Yin, W. Jin and Y. Mu, *Lab Chip*, 2024, **24**, 4659–4668.
112 G. Xing, Y. Shang, X. Wang, H. Lin, S. Chen, Q. Pu and L. Lin, *Biosens. Bioelectron.*, 2023, **220**, 114885.
113 X. Xiang, X. Ren, Q. Wen, G. Xing, Y. Liu, X. Xu, Y. Wei, Y. Ji, T. Liu, H. Song, S. Zhang, Y. Shang and M. Song, *Anal. Chem.*, 2024, **96**, 6282–6291.
114 D. Huang, D. Ni, M. Fang, Z. Shi and Z. Xu, *Anal. Chem.*, 2021, **93**, 16965–16973.
115 C. Wu, Y. Yue, B. Huang, H. Ji, L. Wu and H. Huang, *Talanta*, 2024, **269**, 125414.
116 X. Xiang, M. Song, X. Xu, J. Lu, Y. Chen, S. Chen, Y. He and Y. Shang, *Anal. Chem.*, 2023, **95**, 7993–8001.
117 B. Shu, J. Yang, W. Chen, X. Li, Y. Xue, M. Liu, X. Yin, L. Xu, H. Zhang, J. Qiu and H. Zheng, *Chem. Eng. J.*, 2024, **496**, 154174.
118 N. Zhang, L. Wang, X. Deng, R. Liang, M. Su, C. He, L. Hu, Y. Su, J. Ren, F. Yu, L. Du and S. Jiang, *J. Med. Virol.*, 2020, **92**, 408–417.
119 J. Dronina, U. Samukaite-Bubniene and A. Ramanavicius, *J. Nanobiotechnol.*, 2021, **19**, 348.
120 Z. Liu, W. Naz, T. Yousaf, J. Sun, Q. Wu, M. Guo, G. Tian and G. Sun, *Commun. Biol.*, 2025, **8**, 1030.
121 A. Cassedy, A. Parle-Mcdermott and R. O'Kennedy, *Front. Mol. Biosci.*, 2021, **8**, 637559.
122 F. Nafian, S. Nafian, B. Kamali Doust Azad and M. Hashemi, *Mol. Biotechnol.*, 2023, **65**, 497–508.
123 N. L. Welch, M. Zhu, C. Hua, J. Weller, M. E. Mirhashemi, T. G. Nguyen, S. Mantena, M. R. Bauer, B. M. Shaw, C. M. Ackerman, S. G. Thakku, M. W. Tse, J. Kehe, M.-M. Uwera, J. S. Eversley, D. A. Bielwaski, G. McGrath, J. Braidt, J. Johnson, F. Cerrato, G. K. Moreno, L. A. Krasilnikova, B. A. Petros, G. L. Gionet, E. King, R. C. Huard, S. K. Jalbert, M. L. Cleary, N. A. Fitzgerald, S. B. Gabriel, G. R. Gallagher, S. C. Smole, L. C. Madoff, C. M. Brown, M. W. Keller, M. M. Wilson, M. K. Kirby, J. R. Barnes, D. J. Park, K. J. Siddle, C. T. Happi, D. T. Hung, M. Springer, B. L. MacInnis, J. E. Lemieux, E. Rosenberg, J. A. Branda, P. C. Blainey, P. C. Sabeti and C. Myhrvold, *Nat. Med.*, 2022, **28**, 1083–1094.
124 S. Hameed, L. Xie and Y. Ying, *Trends Food Sci. Technol.*, 2018, **81**, 61–73.
125 C. Deusenbery, Y. Wang and A. Shukla, *ACS Infect. Dis.*, 2021, **7**, 695–720.
126 X. Shi, U. Kadiyala, J. S. VanEpps and S.-T. Yau, *Sci. Rep.*, 2018, **8**, 3416.
127 J. Dietvorst, L. Vilaplana, N. Uria, M.-P. Marco and X. Muñoz-Berbel, *TrAC, Trends Anal. Chem.*, 2020, **127**, 115891.
128 Y. Huang, Y. Lu, X. Liu, M. Chai, L. Yang, K. Yin, J. He, Z. Wang, Y. Zhang, Y. Yu, S. Qiu, Y. Fan and Z. Li, *Sens. Actuators, B*, 2025, **436**, 137612.
129 Y. Hou, Z. Liu, H. Huang, C. Lou, Z. Sun, X. Liu, J. Pang, S. Ge, Z. Wang, W. Zhou and H. Liu, *Adv. Funct. Mater.*, 2025, **35**, 2411484.
130 J. Gupta, S. Saquib abullais, R. H. Althomali, D. Margoth Guanga Chunata, S. Shukhratovich Abdullaev, H. E. Yeslam, O. Sarsembenova, M. F. Ramadan, A. Alsalamy and S. Alkhayyat, *Microchem. J.*, 2023, **194**, 109268.
131 W. Fang, J. Wu, M. Cheng, X. Zhu, M. Du, C. Chen, W. Liao, K. Zhi and W. Pan, *J. Biomed. Sci.*, 2023, **30**, 42.
132 K. K. Hussain, D. Malavia, E. M. Johnson, J. Littlechild, C. P. Winlove, F. Vollmer and N. A. R. Gow, *J. Fungi*, 2020, **6**, 349.
133 S. Puri, S. Shingh and P. Tiwari, *Int. J. Appl. Sci. Biotechnol.*, 2019, **7**, 298–303.
134 R. L. Latham, J. T. Boyle, A. Barbano, W. G. Loveman and N. A. Brown, *Essays Biochem.*, 2023, **67**, 797–809.
135 L. E. Johns, D. P. Bebber, S. J. Gurr and N. A. Brown, *Nat. Food*, 2022, **3**, 1014–1019.
136 S. Zhou, L. Xu, H. Kuang, J. Xiao and C. Xu, *Analyst*, 2020, **145**, 7088–7102.
137 X. Shkembi, M. Svobodova, V. Skouridou, A. S. Bashammakh, A. O. Alyoubi and C. K. O'Sullivan, *Anal. Biochem.*, 2022, **644**, 114156.
138 Y. Zhang, Y. Cheng, C. Zhao, J. Chen, Z. Wu, J. Wang and D. Wang, *Chem. Eng. J.*, 2025, **503**, 158452.
139 Q. Chen, T. Tian, E. Xiong, P. Wang and X. Zhou, *Anal. Chem.*, 2020, **92**, 573–577.
140 Y. Jiang, Y. Wang, W. Luo, X. Luan, Z. Zhang, Y. Pan, B. He, Y. Gao and Y. Song, *Lab Chip*, 2025, **25**, 49–56.
141 Y. Wang, S. Feng, X. Wang, C. Tao, Y. Liu, Y. Wang, Y. Gao, J. Zhao and Y. Song, *Lab Chip*, 2024, **24**, 3521–3527.

© 2025 The Author(s). Published by the Royal Society of Chemistry